The authors are grateful for the thoughtful comments given by the two anonymous referees on our paper. Below, we respond to each point raised by the reviewers and explain the changes we've made to the manuscript accordingly. The reviewers' comments are shown below in italics writing while our response is indicated in a red font.

Anonymous Referee #1

Received and published: 4 March 2020

We are grateful for the first referee's efforts in reviewing the manuscript. We believe our paper has significantly improved as a result of his/her comments. Below, we highlight our responses to the general and specific comments and explain the revisions we've made to the paper accordingly.

General comments

The paper by Hailegeorgis et al. examined upwelling and transport patterns in the Canary Current System using a Lagrangian modeling approach. The authors identified latitudinal variability in water and nitrogen export, determined transit time of water parcels from the coast to the oligotrophic oceanic region, examined the role of major capes as drivers of upwelling and offshore transport, and quantified the coastal upwelling contribution to the nitrogen stock in the North Atlantic Tropical Gyral and the North Atlantic Subtropical Gyral East. Overall, I think that the paper does an interesting contribution to the understanding of nitrogen export patterns in the Canary Current System. However, important changes need to be made in order to recommend publication.

My main concerns are two:

1) The paper is not easy reading:

There are a lot of results and figures with multiple panels and supplement figures, which made fuzzy the paper's main points. There is some redundancy in the reported results. Subregional patterns not always showed important differences, so not sure if you always need reporting all subregional results in the paper main body (you can move some Figure's panels to the Supplement).

In order to solve the redundancy and lengthiness issues in the main paper, we have merged some subsections as well as moved some figures/panels to the supplementary. More specifically:

- We have moved the model validation (including Figs. 1, 2 and 3, which are now Figs. S1, S2 and S16) into the Supplementary section following the reviewer comment 6.
- We have merged subsections 3.1 and 3.2 so there is now no subsection in Section 3.
- We have merged Figure 5 and Figure 6 in one single figure (now Figure 2) and moved some of their sub-panels to a figure in the supplementary (now Figure S22, SI).
- We have merged and consolidated subsections 4.4 and 4.5 into one subsection 4.4 titled "Structure of offshore transport", which includes results on depth structure and horizontal

structure of the offshore transport. We have also brought a figure on the depth structure of offshore transport from the supplementary material to this subsection (now Figure 6).

- Figure 9 has been moved to the supplementary (now Figure S23, SI) as suggested by the reviewer (see below).
- Figure 10 panels c-h has been moved to the supplementary (now FIgure S24, SI).
- We have merged Figure 10 (panels a-b) and Fig 11 into one figure (now Figure 7).
- We have moved most of Section 7 including Table 5 (now Table S4) to the supplementary section, while we kept in the main paper a brief summary of the comparison between our results and previous studies.

2) The manuscript length could be reduced, trying a better integration of the paper results. Results and discussion were mixed, which did not help to get the present study contribution.

We have significantly shortened the paper and consolidated multiple sections (please see our response to previous comment).

I am not an English native speaker, but below (specific comments) I made a series of suggestions to help making sentences more concise and clear.

3) The authors need explaining much clearly how all the Lagrangian patterns were calculated in the Method section.

We have moved some important details of the Lagrangian experiment from the supplementary text into Section 2.2.

We have also improved the description of the Lagrangian experiment by adding a schematic to the supplementary (now Figure S18, SI) that summarizes the different steps followed to quantify the Lagrangian offshore transport (also shown below).

Step 1 Transport driven particle release (ARIANE Quantitative Experiment)	Step 2 Particle tracking (ARIANE Qualitative Experiment)	Step 3 Upwelling identification
The particle release strip is set 50km westward of the 200m bathymetry isobath to be the western boundary of the coastal upwelling domain Particles are released at each vertical cell along the particle release strip on each day of one year of the experiment according to the coastward transport, where each particle is associated with 0.01 Sv of transport or less Particle trajectories are terminated at 720 days or when they exit the coastal upwelling area (whichever comes first) – we call this **exiting the coast**. This domain is limited to the area between the particle release strip and the West African coast. For each particle, its associated volume, position, time, velocity and nearby tracer concentration are saved at its entry into the coastal domain and on its exit from the coast Note that there may be **double-counting** of a water mass that occurs if a water mass enters the coastal domain (initiating release of one particle), exits the coast and re-enters (initiating release of a second particle)	Particle trajectories are initialized at the initial conditions in the quantitative experiment (Step 1) Trajectories are tracked for 720 days or until a particle leaves the experiment domain (whichever happens first) – we call this **exiting the domain**. This includes the whole experiment domain as opposed to the coastal upwelling area in the quantitative experiment. Trajectory information (incl. position, velocity, nearby tracer concentration) is saved on a 1-day interval In the case of a double-counted water mass (see Step 1), it is represented by two particle trajectories starting from its re-entry into the coastal domain	All particles that cross 70m depth (the base of the euphotic zone) upwards while still in the coastal domain (before exiting the coast) are considered **upwelled particles** For all upwelled particles, their trajectories (obtained in Step 2) are considered from their upwelling until they exit the domain In order to account for an upwelled water mass that is double-counted (see Steps 1 & 2), if an upwelled particle leaves the coastal domain but later re-enters and re-upwells, its trajectory since its second upwelling will be discarded (the particle's time of exiting the domain is shortened). This is because the subsequent trajectory will have been considered as an upwelling of a separate particle released at the water mass's re-entry into the coastal domain.

We then added details on ARIANE's quantitative and qualitative experiments from what used to be in the supplementary text. As part of the quantitative experiment, we explained how we save the initial condition (including associated volume) of a particle release and mentioned many important details including the particle release period of one year, the release of particles over all the cells along the particle release strip, the maximum volume associated with particles, etc (please see lines 10-20, page 7). As part of the qualitative experiment, we explained details including the maximum length of trajectories and the frequency at which they are saved, the information saved about each particle along its trajectory and the portion of particles that leave the experiment domain early (please see lines 21-28, page 7).
We also indicated in this subsection that ARIANE neglects vertical mixing in its computation of particle trajectories (please see lines 2-3, page 7). Finally, we have added a new plot (now Figure 1b) of trajectories of a small sample of particles, in order to visually illustrate the Lagrangian experiment.

4) Model validation:

The authors need to include vertical sections and vertical profiles from the modeled variables and compare them with observations (WOA sections would be OK). I would like to see whether the vertical patterns in the model outputs have any significant bias. Is the nutricline depth consistent with observed patterns across the model domain? Is the model reproducing well the seasonal *variability in vertical patterns? It is not enough the correlation analysis in Fig. 1 from the Supplement, since well-correlated variables can have important differences in terms of magnitude.*

We agree with the reviewer. We have produced validations of vertical cross sections of temperature, salinity and nitrate (WOA) for each subregion and for each season (from Figure S6 to Figure S14 in the supplementary).

The model generally does a good job in reproducing the vertical variability in observations for all three variables across the different seasons. We have presented our evaluation with more detail under Model Evaluation, which is now presented in the supplementary material.

As examples, the figures below show seasonal validations of vertical cross sections of (from left to right) temperature at 16N, salinity at 25N and nitrate at 30N. Each of these sample plots is taken from a distinct subregion in our experiment.

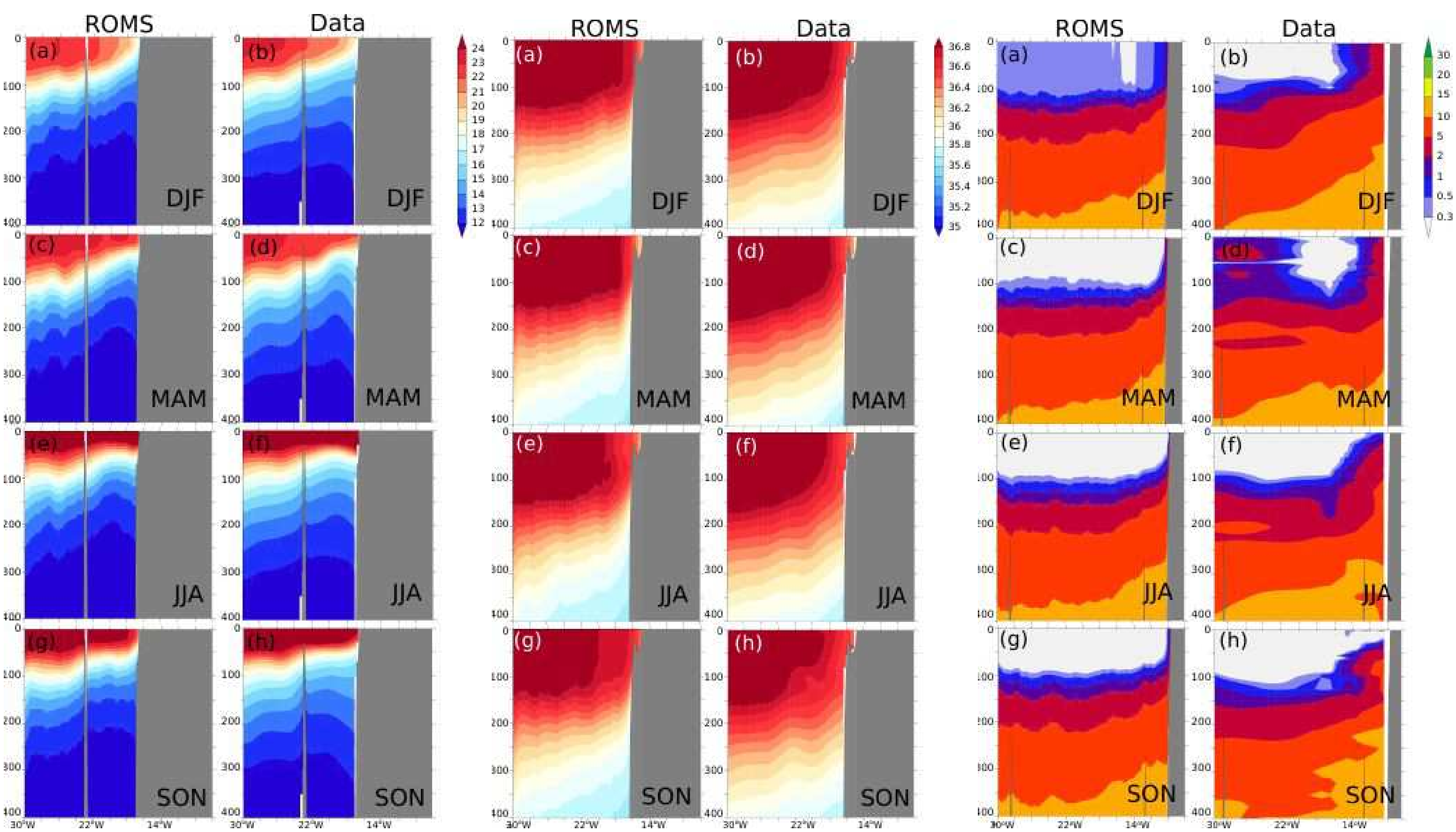

5) Since a correlation analysis per se does not show a potential bias in the simulated variables, besides the annual mean patterns shown in Fig. 2. I would like to see a comparison for mean seasonal patterns of SST and surface chlorophyll.

We have produced seasonal validation maps of SST (Pathfinder) and chlorophyll (SeaWIFS) shown in Figs. S3 and S4 (SI), respectively (shown below, in that order).

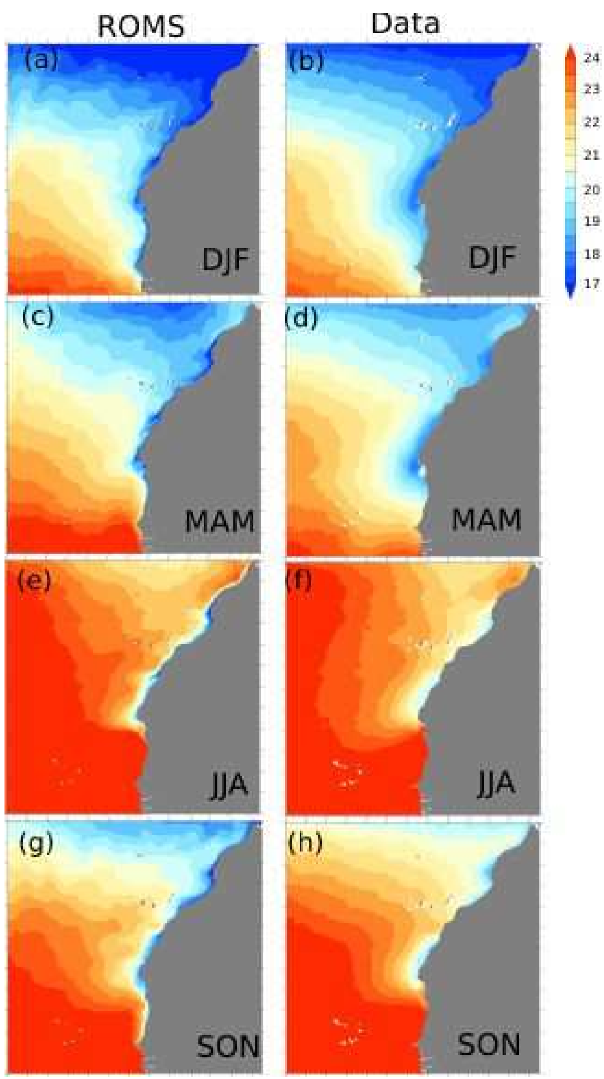

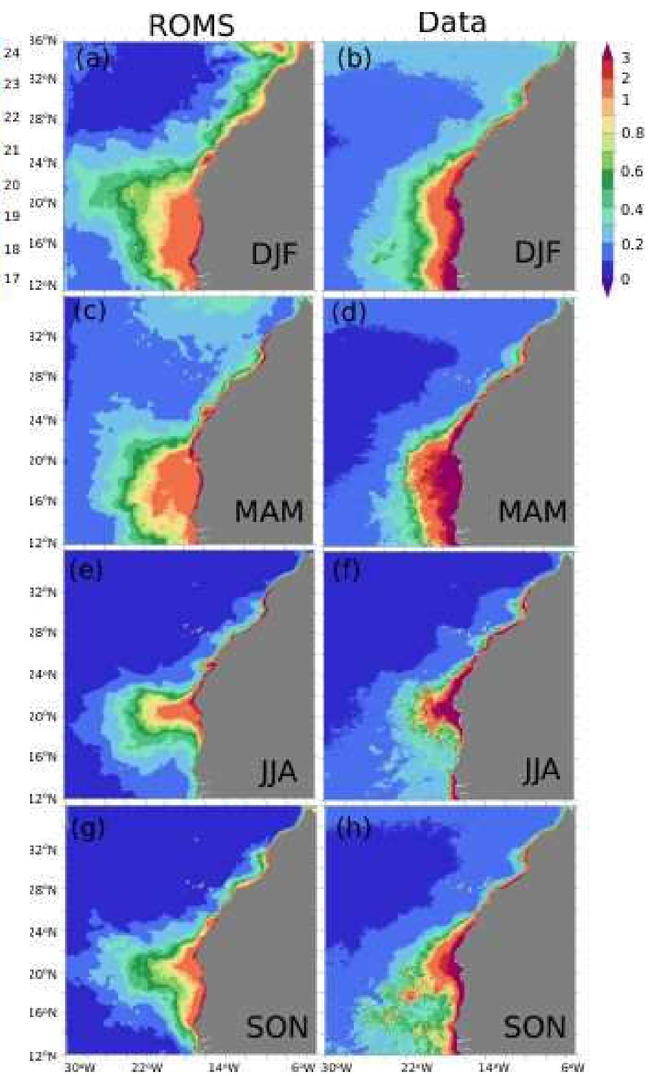

Furthermore, we have added a comparison of modeled mixed layer depth (MLD) to observations in all seasons in Figure S5, SI (please see our response to comment #20)

6) To reduce paper length, I recommend including the model validation as an independent section in the Supplement.

Following the reviewer's suggestion, we have moved the model validation to the supplementary.

Specific comments:

7) Please, refer to the supplement figures as Figure S1, Figure S2, etc. It was confusing when a paper and supplement figures were mentioned at the same time. As example, instead of using (Fig. 7 and Fig. 8, SI), use (Fig. 7 and Fig. S8).

We have made these changes.

8) Abstract
Pag.1, L11: "Our model analysis suggests that the vast majority of the upwelled waters originate from offshore and below the euphotic zone (70m depth), and once upwelled remain in the top 100m". I understand what you mean, but the statement is not clear. Consider that you defined upwelling as a water parcel crossing the 70 m depth level.

The sentence in question has now been removed from the abstract.

9) Introduction
Pag.2, L13-14: The sentence "leading to substantial modifications of the biogeochemical cycles there" is ambiguous. You could delete it.

Done.

10) Pag.2, L20: delete "potentially"

Done.

11) Pag.2, L32: delete "potentially"

Done.

12) Pag.3, L10: "surface jet associated with the upwelling flowing equatorward" => "surface jet associated with the coastal upwelling front, which flows equatorward"

Done.

13) Pag.4, L6: "and therefore did not estimate" => "so did not estimate".

Done.

14) Pag.4, L8-10: These sentences need additional work. Explain better but concise.

When it comes to the quantification of the contribution of the Canary upwelling to the open ocean nitrogen budget, the Lagrangian approach presents a couple of advantages relative to the Eulerian approach. Because of its focus on water particle trajectories, Lagrangian tracking of water masses is better suited for the analysis of connectivity between the coastal and the open ocean regions. Furthermore, the Lagrangian method can be used to derive conditional statistics where subsets of particles that fulfill certain criteria are analyzed. This is useful for instance to restrict the analysis of offshore transport to upwelling particles only.

This is now better explained in the revised manuscript (please see lines 1-19, page 4).

15) Pag.4, L13: What do you mean with "quantify the reach"

We have modified this to 'quantify the offshore reach' (please see lines 6, page 4).

16) Pag.4, L13: "the spatial structure and the dominant timescales"

Done.

17) Pag.4, L23-24: and quantifying the offshore export

Done.

18) Pag.4, L24: "We also investigate"

Done.

19) Methods
Pag.5, L2: Was bottom remineralization included in the model? This is a relevant source of nitrogen, which can largely influence inorganic nitrogen patterns on the shelf. If it was not considered, you should mention it as another limitation in the study.

Yes, the sinking particulate organic matter that reaches the seafloor is remineralized back into ammonium at a slower rate ($0.003\ d^{-1}$) than in the water column ($0.03\ d^{-1}$ for small detritus and $0.01\ d^{-1}$ for large detritus). We have added that explanation and a reference to Gruber et al. (2006) (please see lines 7-9, page 5).

20) Pag.5, L14-15: Did you use a monthly climatology for wind stress? If this is the case, vertical mixing was probably underestimated. Did you compare the simulated mixed layer depth with observations?

We used a monthly wind climatology (QuickSCAT SCOW). We have added a comparison of the modeled mixed layer depth (MLD) with observations for all seasons (Figure S5, SI). Using a monthly climatology forcing likely contributes to the underestimation of EKE shown (now in Fig S1, SI). We have acknowledged this in the Implications and Caveats (Section 8, lines 21-26, page 25). However, much of the spatial and seasonal variability in upper ocean mixing is still captured by the model as can be seen in the mixed layer depth validation in Figure S5 (shown below). This is particularly true in the summer and fall when the simulated MLD agrees the most with observations. This has been mentioned in the Model Evaluation section in the supplementary material (please see lines 20-22, page 1, SI).

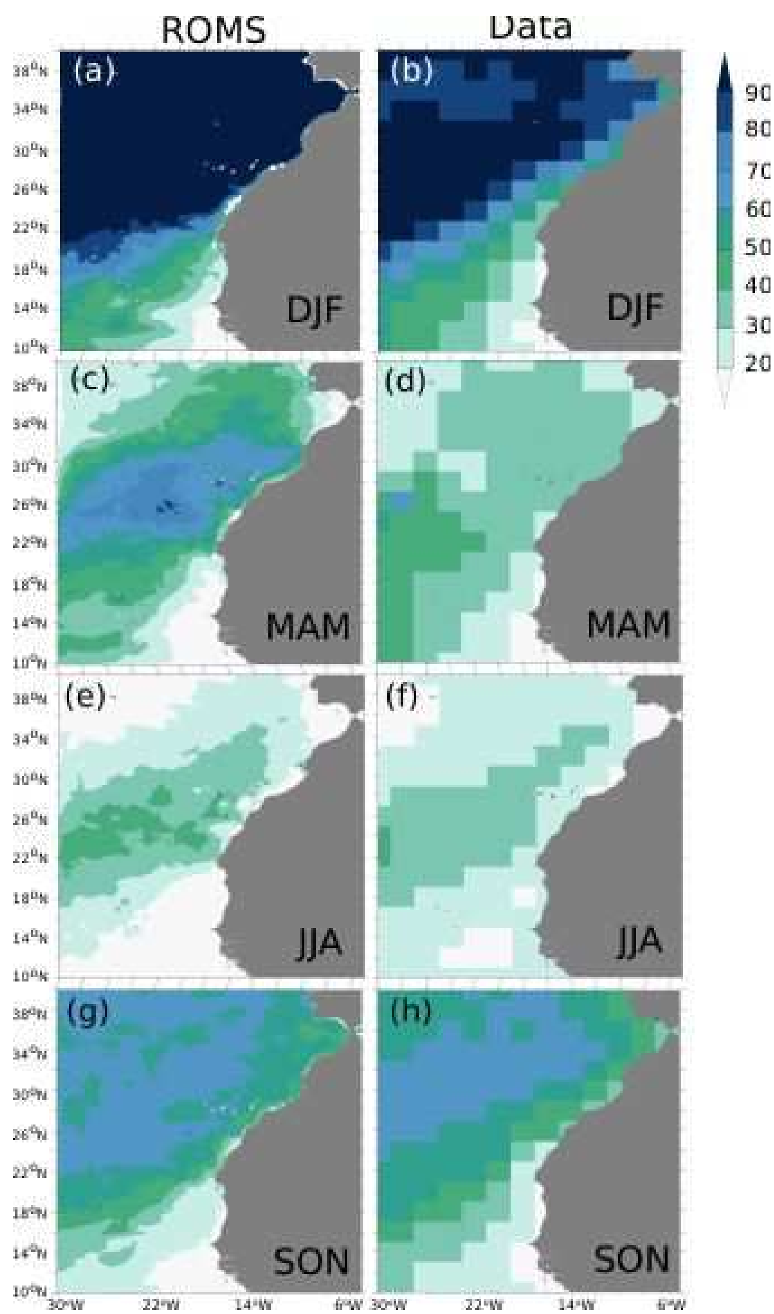

21) Pag.5, L17-18: It was mentioned that the model was spun up by 12 years, and the study was based in simulation years 10 to 12. So does it mean that you used the last 3 years of your model spin up for the analysis? If this is the case, you have to report that the model was spun up by 9 years.

Yes, we did spin up for 9 years then used years 10-12 to run the experiment. This correction has been made (please see lines 20-21, page 5).

22) Figures 1 and 2: I suggest including the 200 m isobath (shelf break) as a contour line on the maps.

This change has been made in the figures in the revised manuscript (see Figs S1 and S2, SI).

23) Pag.9, L2: It is Figure 2 not 1.

Done.

24) Pag.9, L14: Indicate that vertical mixing is not considered in the Lagrangian analysis

This has been clarified (please see lines 2-3, page 7).

25) Pag.9, L25: Since the dominant circulation pattern in the CanCS appears to be along-shore, I am wondering why only oceanic particles were considered in the Lagrangian experiment. I would expect that upwelled particles also come from the northern and southern boundaries. Could the poleward undercurrent be a source for upwelled waters?

It is true that potential upwelling driven by waters entering the coastal zone at 14N and 35N were not included. We have acknowledged this among the study's caveats (please see lines 27-28, page 26).

Our choice to only allow open ocean particle releases was dictated by technical constraints in Ariane that prevent individual segments to be considered simultaneously as entry and exit sections. Yet, in order to quantify the potential error associated with our simplification we have run a separate experiment where particles were allowed to enter the coastal ocean from the southern and northern boundaries of the upwelling strip. Our analysis reveals that we are missing only a very small amount of water by our choice, i.e., only about 1% and 3% of the total volume tracked in this study come through the northern and southern boundaries, respectively.

Furthermore, given the high rate of recirculation near the coast, a vast proportion of the particles that may have entered the coast alongshore, once upwelled and exported offshore, are likely to return to the coast from the open ocean, in which case they would be sampled in our particle release.

We conclude that discarding particles entering the coastal ocean from the southern and northern boundaries of the upwelling strip is likely to cause only a limited error in our quantification of the offshore transport.

We have further highlighted this caveat and discussed its potential implications in Section 8 of the revised manuscript based on the arguments developed above (please see lines 28-34, page 26).

26) Results
Pag.13 L7: "onshore-offshore contrast" => "cross-shore differences"

We have made this change.

27) Pag.13 L9: "followed by a second one at around 50 km from the shore" => "and a secondary maximum around 50 km"

We have made this change.

28) Pag.13, L20. Shallow regions should also show upwelling because a distance of 50 km from the shelf break was considered for the analysis. Right? Clarify.

The reason there is no upwelling at the very coast in these regions is that the bathymetry is shallower than 70m, therefore making it impossible to meet our criteria for upwelling where a particle crosses the 70m depth. The minimum bathymetry allowed by the model is 50 m and that has been added to the model's description in section 2.1 (Page 5, Lines 12-13) as Reviewer 2 has also requested (see below). However, as mentioned by the referee we sample upwelling further offshore in these locations. Therefore, for more clarity we have changed the statement to: "our experiment identifies limited coastal upwelling south of Cape Blanc and between Capes Barbas and Bojador because their bathymetry is shallower than the 70 m upwelling depth criterion used here" (please see lines 21-2217, page 9).

29) Pag.13, L25: what is the range considered for the upwelling zonal integration in Figure 6a (same for Figure 5a).

We integrate zonally across the coastal stripe (Between the coast and 50 km westward of the 200m bathymetry). We have added this clarification to the caption for the panels (now Figure 2).

30) Pag.13, L26-28: Wondering if the shallow nutricline is linked to the high-nutrient SACW or not.

No. The shallow nutricline is a consequence of the shallow thermocline which is caused by the stronger stratification in the tropics in comparison with the high latitudes.

31) Pag13, L28-29: “The central subregion has a moderate nitrogen flux associated with upwelling while the northern subregion has the weakest upwelling flux of nitrogen” => “The weakest upwelling-driven nitrogen flux was in the northern subregion”

We have made this change.

32) Pag.13, L30: “disproportionately lower” => “much lower”

The sentence in question has now been removed in the revised manuscript.

33) Pag.15: It is important to note that a water parcel released in region A can be upwelled in subregion B or C. Beside, a water parcel upwelled in region A can be transported away to region B or C. Consequently, the parcel transport not necessarily depends on the oceanographic conditions in region A. If I’m right, I suggest revisiting all sentences describing subregional offshore transport results. As example, I would modify “the offshore transport is fastest in the central subregion and slowest in the northern subregion” by “the particle upwelled in the central and northern subregions displayed the fastest and slowest offshore transport, respectively”. Besides, I would change “At larger distances from the coast (beyond 400 km), the offshore transport becomes faster in the southern subregion” by “The fastest water parcels beyond 400 km from the coast are those upwelled in the southern subregion”

We have followed this suggestion and corrected the way we express transport from each subregion accordingly. This has been applied throughout the paper.

34) Pag.15, L3: define “transit time”.

We have added here the transit time definition from the caption of Figure 3 in the revised manuscript.

35) Pag.15, L15-16: Why is this maximum at 150 km? Does it mean that a greater fraction of water parcels remains around this distance? Is this linked to patterns in alongshore circulation?

In the revised manuscript, we have added an explanation that the distance of maximum transport corresponds to the distance reached by most sampled upwelled water (nitrogen). It is around 150km (that roughly corresponds to the width of the upwelling stripe) because at closer distances to the coast (<100-150km), upwelled volume is only partially sampled. Farther distances (>100-150km) are never reached by a proportion of particles because of recirculation retaining them close to the coast and alongshore transport exporting some particles out of the model domain (please see lines 5-10, page 11).

36) Pag.15: L22: “This is because of its low offshore transport efficiency and the relatively low volume of upwelling” => ‘’Reduced coastal upwelling and low offshore transport efficiency explain this pattern.”

We have made this change.

37) Pag.15, L22: Define transport efficiency.

Transport efficiency (the ratio of offshore transport volume at a given distance to upwelling volume) has been defined in the revised manuscript (Page 11, Line 16).

38) Table 2: It may be informative reporting the standard deviation for transit time.

We have replaced Table 2 with a graph of transit times featuring error bars (Figure 3 in the revised manuscript).

39) Pag.16, L3-5: “At close to 150 km from the coast (corresponding to the edge of the coastal upwelling stripe), the offshore transport of nitrogen reaches its maximum, reaching values as large as 500 Gmol yr−1. Thereafter, the offshore transport decreases exponentially” => “Around 150 km from the coast, the nitrogen transport reaches values as large as 500 Gmol yr-1 at 200 km, decreasing exponentially further offshore”

We have made this change.

40) Pag.16, L7: “In spite of having the lowest offshore transport of water, the southern subregion exports the highest amount of nitrogen offshore at 200 km” => “Although offshore water transport was minima in the southern CanCS, this subregion has the greatest offshore export of nitrogen.”

We have made this change.

41) Pag.16, L9: “At larger distances from the coast, the situation reverses.” => “This pattern reverses further offshore”

We have made this change.

42) Pag.18, L2-4: I disagree with this statement: “so that beyond the nearshore 50 km region, inorganic nitrogen in the form of nitrate dominates the nitrogen pool at all distances from the coast”. NO3 dominates almost everywhere, and its contribution to total nitrogen is actually much larger in the coastal region than in the oceanic region.

We agree with the referee that NO_3^- dominates nearly everywhere. Yet, in the nearshore 50km region, the sum of all organic nitrogen (in both plankton and detritus forms) can exceed that of nitrate as shown by the fraction of organic N in the offshore transport (red dashed curve) in Figure 5.

43) Pag.18, L21-34: It would be nice having a brief introductory explanation for the motivation of the analysis in this subsection. As example, evaluate the impact of subduction on transit time, impact of subduction on nutrient fluxes or nutrient cycling.

We have added introductory statements in the beginning of this subsection on the potential impact of vertical structure of offshore transport (subduction) on transit times and offshore transport efficiency to serve as motivation for the depth structure analysis (Page 14, Lines 5-7). Later in the subsection, these potential links are revisited based on the analysis that has just been presented (Page 16, Lines 3-5). In general, subduction increases transit times (slows down offshore transport) since velocities deeper in the water column are smaller. However, subduction can also increase the efficiency of offshore transport by minimizing the depletion of nitrogen in surface waters.

In the original draft, we had also related subduction of water particles with filament activity (page 18, lines 30-31) and with nitrogen offshore transport efficiency (Page 31, Lines 18-23; Page 32, Lines 2-4).

44) Pag.18, L21: "Upwelling particles that..." => "Upwelled particles that..."

We have made this change.

45) Pag.18, L22: How do patterns in Fig. 8a,b from the supplement were calculated?

To make Figure 8 a (or b) in SI, we first considered all downward (or upward) movements of all particles across the horizontal plane at 50m depth. After finely binning the horizontal surface across the model, we added the associated volumes of all particles that crossed this depth downward (or upward) for each binned area throughout the 2 year particle trajectory experiment. We have added more detail to the caption of the figure (now Fig. S27) in the Supp. Information to show this more clearly.

Although Fig. 8c in SI gives the dominant vertical transport (upward or downward) in the modeled region, panels (a) and (b) also complement this information by giving the full picture of where the upward and downward transport occurs during the whole 2 year experiment. Panels (a) and (b), for example, show that although the coast is dominated by an upwelling flux, it also features significant downwelling.

46) Pag.18, L24: I cannot see the secondary upwelling in the open ocean. Describe better.

It is true that Figure 10d in the submitted manuscript doesn't show significant upwelling flux for particles upwelled in the southern subregion except for a subsurface upward transport maxima in the first 300km from coast. So we now only cite Figure S27(c) in the revised supplementary material, which does show strong net upward transport (upwelling) in the open ocean in the southern CanCS, which has significant overlap with the trajectory of the upwelling from this subregion.

47) Pag.18, L30: It is not evident for me why persistent filaments contribute to enhanced subduction. Explain.

Here, we were referring to the role of filaments in squirting cold upwelled water offshore and the subsequent subduction of this cold water due to its high density compared to the open ocean's warmer surface water. We have now added a sentence stating this fact including a reference to Lovecchio et al. (2018), who found filaments to cause subduction of organic nitrogen, for example, to depths larger than 100m (Page 14, Lines 13-15, in the revised manuscript).

48) Figure 9: I recommend include this figure in the Supplement.

We have made this change.

49) Pag.20. Indicate what the positive/negative values in Fig. 10 represent

We have made this change.

50) Pag.21. Indicate what the positive/negative values in Fig. 11 represent

We have made this change.

51) Pag.22, L26: "offshore transport of upwelled particles"

We have made this change.

52) Pag.22, L30: I am not sure whether remotely upwelled water is a good term. I would prefer describing the results in terms of local and non-local upwelling.

We have changed all references to "remote upwelling" to "non-local upwelling".

53) Pag. 22, L32: "water upwelled"

We have made this change.

54) Pag. 23: L1: “Corresponding enhancement in local nitrogen upwelling and export is seen only in” => “Increased offshore transport of nitrogen due to increased local upwelling is seen only in”

We have made this change.

55) Caption of Figure 12: “Transport by water upwelling locally” => “Transport associated with locally upwelled water”
“Transport by particles that leave the coastal upwelling region at each cape or non-cape area but upwell remotely” => “Transport associated with remotely upwelled water”

We have made these changes. We have slightly modified the second edit suggested by the referee to “Transport associated with non-locally upwelled water at each cape or non-cape area”.

56) Pag.24, L1-2: “The offshore transport of nitrogen by remote upwelling exported by all capes constitutes more than 30% of the total offshore transport of upwelling” => “Remotely upwelled waters that are transported offshore around major capes represent more than 30% of the total transport”

We have made this change.

57) Pag.24, L4-5: “In fact, all capes source the majority of water and nitrogen they export from remote upwelling (Table 3). All capes also source more of their export from remote upwelling compared to the rest of the coast.” => “Indeed, most of the water and nitrogen exported offshore around major capes is non-locally upwelled (Table 3)”

The second sentence is meant to show the high export of non-local upwelling that occurs at capes compared to the non-cape coast. But the phrasing was unclear so we have modified it slightly to: “Each cape also sources more of its export from non-local upwelling than any of the non-cape coastal areas.” (Page 17, Line 21).

58) Pag.27, L10: For consistency use CanCS

We have made this change.

59) Pag.27, L21-29: I did not understand. Please, explain better how did you estimate the CanCS contribution to the NATR and NASE provinces.

We have added a brief clarification of our calculation to the footnote of Table 3 in the revised manuscript. Briefly, it is as follows.

We explain that whenever a particle enters a province within the top 100m, the nitrogen it carries into the province is added to the particle's source subregion's contribution to the province. On the contrary, when a particle from a given subregion leaves a province within the top 100m, the nitrogen it carries with it when it leaves the province is subtracted from the contribution of the subregion of the particle to the province.

We use precise Longhurst province boundaries for our analysis. Analysis of crossing into and out of a province is determined based on a daily resolution of particle positions since that is the resolution of our Lagrangian trajectories.

[[[[[///// \\\\\

Anonymous Referee #2
Received and published: 5 March 2020

We would like to thank the second reviewer for the comments that have, we hope, significantly improved our manuscript. Below, we highlight our responses, point by point, to the reviewer's general and specific comments and indicate the revisions we have made to the paper accordingly.

General comments

This study aims to determine the contribution of nitrogen upwelled within the coastal region of the Canary Upwelling System to the nitrogen budget of the open ocean through a Lagrangian study relying on model outputs generated by a coupled physical-biogeochemical experiment. Authors also aim at describing the timescales, the reach and the structure of this offshore transport to quantify the role played by upwelling on nitrogen enrichment of the NATR and NASE provinces as defined by Longhurst. I'm not sure the study makes a significant contribution to the issue of nitrogen irrigation of the NATR and NASE provinces. There are several reasons for this.

1) *First, the authors justify the originality of their study by the use of a Lagrangian approach as opposed to Eulerian approach which has been used in Auger et al. (2016) or Lovecchio et al. (2017, 2018) which have been mentioned in the present study. The authors in particular advance the capacity of their Lagrangian approach to define more faithfully the contribution of the coastal upwelling region in terms of nitrogen supply to the subtropical gyre (l5-10, page 4). This statement seems relevant with regard to the volume transported from the coastal region to the open sea, but much less obvious with regard to the transport of nitrogen. Indeed, the amount of nitrogen carried by each particle to a given location is quantified as the product of the particle associated volume and the concentration of the tracer associated with the particle when it reaches that location (l4-6*

page 11). To my understanding of the methodology, the nitrogen concentration at a particular location does not necessarily come from the coastal upwelling but can be supplied locally, can change its chemical form or have a different origin.

We do agree with the referee that in contrast to water volume, tracing the transport of nitrogen is somewhat more difficult given the chemical transformations between inorganic and organic nitrogen. In addition, subgrid mixing is not represented in our Lagrangian particle tracking but can affect nitrogen concentrations in ways that are not accounted for in our transport estimates.

Yet, as has been shown also by Frischknecht et al. (2018), the Lagrangian method permits a lot of new insight into the offshore transport of nitrogen, since total nitrogen, i.e., the sum of inorganic and organic nitrogen is conserved except for the part that is sinking, and that part that is being supplied through mixing. Indeed, along the way, nitrogen can be incorporated into organic matter and then being recycled again, but if it is tracked by our algorithm, this nitrogen is still coming from the coastal upwelling.

The component we lose through sinking does not affect our conclusions, since this component is lost to the ocean interior, from where it will not find its way back into the waters that are transported offshore. More importantly is our lack of consideration of the vertical mixing. We have good evidence that this component is relatively small. First, the total amount of nitrogen is decreasing with offshore distance, and not increasing. In fact, the decrease is driven entirely by the sinking component, and the spatial distribution of this loss fits well the spatial distribution of the export of organic nitrogen (Figure 4 in the revised manuscript). In particular, we see a decline in total nitrogen as a function of distance to the coast that is sharper than for water volume. And this decline is larger for water particles originating from the southern subregion that are transported at the shallowest depths (Figure S23 in the revised SI). If the supply of nitrogen from surrounding waters to upwelling waters due to mixing were large enough to cancel the loss due to organic matter sinking, there would be no such a sharp decline in the offshore transport of nitrogen as a function of distance to coast. This suggests that although the potential changes in nitrogen due to subgrid mixing can locally be important, they are unlikely to affect the large-scale transport estimates in a significant way.

Yet, we acknowledge that the lack of a representation of mixing in Ariane is an important caveat that not only can affect particles' depth, but also potentially their nitrogen content and hence locally our offshore transport estimate. This is now explicitly stated in the discussion of the method caveats (Section 8, Page 25 (Line 34) to Page 26 (Line 16)).

2) *In addition, authors indicate some limitations of the biogeochemical model (absence of colimitation, absence of nitrogen fixation; l30-34, p31) but omit the potential role of different communities of phytoplankton. Indeed, the model used only represents a single phytoplankton community, the representation of diatom organisms (comprising a siliceous skeleton and likely to contribute significantly to the export of organic matter) could influence the export in the model. In*

terms of export, it has also been shown that the alternation of phase of intensification and relaxation of the upwelling favorable winds is important for the dynamics of the upwelling systems (significant efflorescence generation and sedimentation). The use of climatological wind in this study is likely to play a role in the results because it does not represent these alternations. These aspects should be mentioned in the limitations of the study.

We agree that similar to other state-of-the-art models, our model (especially the biogeochemical module) has other limitations beyond what we have already acknowledged in the original version of the manuscript. Yet, the fact that the simulated (1) distributions of nitrate and its seasonality (Figs S12, S13, S14) and (2) the POC vertical profile (Fig S15) agree relatively well with the observations suggests that the impact of these limitations on the study conclusions is likely limited. See also our response to comment 4 by Reviewer 1.

Nevertheless, following the referee's suggestions we have added two additional potential model limitations in the caveat section (Section 8): 1) the fact that the model does not represent multiple phytoplankton groups and 2) the use of climatological winds lacking high-frequency variability that may lead to a misrepresentation of some aspects of the complex upwelling dynamics (please see lines 21-26 and lines 29-31, page 25).

3) *Then, the conclusions of the study highlight the importance of the Capes in the generation of filaments which represent privileged export sites but the influence of topographic accident on the generation of filaments has already been studied theoretically (eg Meunier et al., 2010), through hydrodynamic simulations and observations for certain filaments of the Canary upwelling system. The quantification of the overall contribution of filaments and the extension of the source waters supplying the main filaments of the system nevertheless provides interesting information, even if the three-dimensional dimension of upwelling is becoming more and more essential in the literature targeting these upwelling regions.*

We agree with the referee in that previous studies like Meunier et al. (2010) and Troupin et al. (2012) have demonstrated the importance of coastal topography and capes in particular in the formation of coastal filaments. Therefore, we have added references to these previous works in the revised manuscript.

In particular:

- we have changed the statement in the original manuscript:"Coastal filaments along the West African coast can occur everywhere, but it is well established that the majority of the filaments are persistently associated with the major capes along the coast" (Page 22, Line 14) to "Coastal filaments can occur everywhere anywhere on the coast in the CanCS, but previous studies have shown that capes can facilitate their formation (Meunier et al., 2010; Troupin et al., 2012)" (Page 16, Lines 23-24 in the revised manuscript).
- to the list of citations on page 24, line 10 in the original manuscript, we have added Meunier et al. (2010) and Troupin et al. (2012) to highlight that the alongshore advection can

interact with capes to result in the formation of a coastal filament that then exports upwelled water to the open ocean (Page 17, Lines 27-29 in the revised manuscript).

4) *The role of mesoscale activity on residence times and the kinetics of transport from the coastal zone to the open sea is also part of the presented results. Mesoscale activity in the transition zone has been widely studied in all eastern boundary upwelling systems and fairly exhaustively in the northern part of the Canary system, in particular from the ROMS model (Mason et al., 2011 & 2012 ; Troupin et al., 2012).*

We agree that previous studies mentioned by the referee have studied the mesoscale variability in the northern Canary system. We have added references to these papers in the revised manuscript.
In particular, we now cite:

- Mason et al. (2011) in section 5.2 among the papers we cite to refer to mesoscale variability and overall transport complexity in the Canary (line 1-3, page 20).
- Mason et al. (2012) in our literature review in the introduction section and section 5.2 on recirculation (line 22-23, page 4; line 1-3, page 20).
- Troupin et al. (2012) in our description of the Cape Ghir filament (line 25-29, page 16).
- Barton and Aristegui (2004) on mesoscale activity in the Canary (see subsection 5.2, line 1-3, page 20).

5) *In the southern part of the area studied, the underestimation of EKE (Figure 1), an activity also highlighted by the occurrence of eddies in this region (Schutte et al., 2016), is not mentioned and is likely to impact the results in this region. The literature on the region is also to be completed, in particular to take into account recent studies by German, Senegalese and French teams. This update particularly concerns the southern part of the system which would allow the authors to describe their results more precisely. Hydrological conditions off Mauritania are described in Klenz et al. (2018), the vortex activity is studied in Schütte et al. (2016), the understanding of the dynamics of the Mauritanian current was revisited by Kounta et al. (2018), and the functioning of the Senegalese upwelling by Ndoye et al. (2014, 2015, 2017) or Capet et al. (2017). These studies point in particular to the importance of the Mauritanian current (to which I prefer the name West Africa Boundary Current; Kounta et al., 2018) on the dynamics of upwelling.*

We agree with the referee that the model underestimates the EKE in the coastal area of the southern subregion, and particularly so south of Cape Verde. Following the referee's comment, we now explicitly mention the underestimation of the EKE in that region and its potential implications among the study's caveats (Section 8, line 21-26, page 25).

Following the referee's suggestion, we also have expanded our review of the literature in the region. In particular, we have cited the following works in the revised manuscript:

- Schutte et al. (2016) and Kounta et al. (2018): are cited in subsection 5.2 (as well as in the Introduction section) to highlight the potential importance of the Mauritanian current and eddies in the region in fueling offshore export of water (please see lines 9-11, page 3; line 1-3, page 20; lines 5-6, page 21).
- We also cite Glessmer et al. (2009) and Peña-Izquierdo et al. (2015) to emphasize the importance of the Mauritanian current in the Introduction section (please see lines 9-11, page 3).
- Klenz et al. (2018): is now cited in section 5.1 to highlight the importance of both the poleward (Mauritanian) current as well as the equatorward Northern Atlantic (Canary) current, particularly during winter, as a source of upwelling in the southern subregion. This helps explain the patterns in Figure 13 (now Figure 9 in the revised manuscript) for the source waters of exports at capes in the southern subregion (please see line 31-32, page 17).
- Ndoye et al. (2017) and Capet et al. (2017): have been cited in our description of the Cape Verde filament and the importance of the local mesoscale activity in section 5.2 (please see lines 25-29, page 16; lines 1-3, page 20; lines 5-6, page 21).

6) *Finally, questions remain as to how to assess the contribution of nitrogen from coastal waters to new production. Indeed, I did not understand the use of VGPM models to quantify primary production knowing the large differences that exist in satellite-based models of primary production in the region (Gomes-Letona et al., 2017).*

We used satellite-based (VGPM) NPP estimates because of their synoptic-scale coverage, which individual in-situ estimates lack. However, we are aware of the important uncertainties associated with this (and other satellite-based) product(s). Therefore, we have now added productivity estimates based on in-situ measurements that are available for some Longhurst provinces (Tilstone et al., 2009) as well as estimates from the CbPM model (Westberry et al., 2008).

Indeed, in-situ estimate of primary production for the NATR based on Carbon-14 uptake from Tilstone et al. (2009) has been added. This estimate (1377mmol N m-2 yr-1) is less than that derived from satellite data (1753 mmol N m-2 yr-1). This suggests that the contribution of the Canary upwelling nitrogen supply can be locally even more important in relative terms, than what our initial estimates have implied. Using a carbon-based productivity model (CbPM), NPP estimates for the NATR and NASE both amount to around 2000 mmol N m-2 yr-1. This also suggests that the CanCS's contribution to the NASE is locally more important than what the province's VGPM value (2139 mmol N m-2 yr-1) suggested.

We have updated Table 4 (now Table 3) and the discussion of the potential contribution of the nitrogen transport to the total NP estimates in the NATR and NASE provinces accordingly (please see lines 10-13, page 23; lines 22-24, page 23). In the table, we now don't show the NPP values but only the NP value range derived as a product of these NPP values and the ef-ratios.

Finally, Gomez-Letona (2017) compares three alternative estimates of PP and finds divergences between them. However, their estimates and comparisons are focused on the coastal area while we were primarily interested in finding estimates for the larger adjacent Longhurst provinces so that we could compare offshore transport of nutrients in our model with the provinces' total budgets.

7) *The manuscript is however well written, well illustrated with clean and condensed figures, the methodology is well described, and the main messages are clearly presented.*

We thank the referee for his/her positive and encouraging comment.

8) *As a summary, the manuscript is of good quality but I hardly consider the results as really moving our understanding forward. The methodology that uses Ariane as a Lagrangian tool is supposed to make a difference in the description, quantification of nitrogen irrigation of NATR and NASE provinces but I'm not convinced that it solves the issues faced by an Eulerian approach.*

Again we thank the referee for praising the quality of the manuscript. We believe that while it comes with important limitations, our study does improve the quantification of the coastal upwelling supply of nitrogen to the open ocean, relative to the Eulerian approach. We detail our reasoning in our response to the previous comment #1 by the same reviewer.

Specific comments

9) *L21-23, page 2: Reformulate the sentence "Especially low-latitude ..." which is hardly understandable.*

We have made this change (please see lines 15-17, page 2).

10) *L12, page 3: The current of Mauritania must be considered in the light of the work of Kounta et al. (2018).*

Done. See response to comment 25 above.

11) *L30, page 4: Did you use ROMS or CROCO oceanic modeling system?*

We used ROMS-AGRIF version 3.1.1 (which shares the same code with the current version of CROCO).

12) *In this section 2.1.1, indicate the shallowest depth used at the coast (hmin parameter).*

We have now indicated the 50m lowest bathymetry in section 2.1 accordingly (please see lines 12-13, page 5).

13) *L26-28, page 5: EKE in the southern part of the domain is underestimated, please tell it and justify it.*

We indicated in the revised manuscript that the model underestimates EKE in the southernmost part of the CanCS region as well (Section 8, lines 21-22, page 25).

14) *L30-31: A warm bias seems to occur in the south, maybe a map of SST differences would make biases straightforward for the reader.*

We have included a map of SST difference that indeed shows a positive bias of less than 1C in the southern part of the domain (Figure S2, Supp. Info).

15) *Figure 1: Arrows on a) and b) are almost invisible.*

This has been corrected.

16) *Figure 2: Validation on annual field does not inform on the ability of the model to correctly simulate the upwelling occurring in the southern part of the domain at the winter-spring time of the year. I believe it would strengthen confidence on the simulation to add this component.*

Seasonal evaluation figures have been added for sea-surface temperature, sea surface cholorophyll, mixed layer depth as well as vertical sections of temperature, salinity and nitrate in Figures S3 to S14, SI (see also our response to comments 4 and 25 by referee #1).

17) *L6-7, page 11: Why not telling here why you chose 70 m depth as upwelling criteria rather than explaining the reason much later.*

We have moved our justification for using the 70m depth here (page 7, line 29-30).

18) *L14-15, page 13: the description of the upwelling does not fit with the dynamic of the upwelling in the southern part of the domain (Ndoye et al., 2014, 2015, 2017; Capet et al., 2017)*

We have corrected this statement to" "Similarly, the Ekman-driven upwelling in the southern subregion is restricted to the winter and spring (Pelegri and Benazzouz, 2015; *Capet et al., 2017*)" (please see lines 15-16, page 9).

19) *L4, page 18: rather 300 km than 200 ?*

This has been updated to 300km (please see line 21-22, page 12).

20) *Section 6: NPP and regenerated production are calculated by the coupled model. Why authors use satellite-based models here?*

Data-based NPP estimates are used because the model domain covers only partially the NASE and NATR provinces. We have added new in-situ based NPP estimates from Tilstone et al. (2009) and a new satellite-based NPP product (Westberry et al., 2008) (please also see our response to previous comment (6)).

21) *L31-34, page 31: Authors indicate some limitations of the biogeochemical model (absence of colimitation, absence of nitrogen fixation; l30-34, p31) but omit the potential role of different communities of phytoplankton. Indeed, the model used only represents a single community of phytoplankton, the representation of diatom type organisms (comprising a siliceous skeleton and likely to contribute significantly to the export of organic matter) could influence the export in the model. In terms of export, it has also been shown that the alternation of phases of intensification and relaxation of the upwelling favorable winds is important for the dynamics of the upwelling systems (blooms and sedimentation). The use of a climatological wind in this study is likely to play a role in the results because they don't represent these alternations.*

We acknowledge two additional model limitations in the caveat section: 1) the fact that the model does not represent multiple phytoplankton groups and 2) the use of climatological winds lacking high-frequency variability that may lead to a misrepresentation of some aspects of the complex upwelling dynamics (please see lines 21-26 and lines 29-31, page 25). Yet, the fact the model is able to represent the observed large-scale distribution of nitrate and its seasonality as well as the vertical mean POC profile (in the original and validation figures and Figs S12-S15, SI) suggests that the impact of these limitations on the study conclusion is limited. It is also important to note that when it comes to the issue of offshore transport, the specific nature of the phytoplankton community is of secondary importance. What matters much more is the role of dissolved organic matter, whose production could be related to phytoplankton community structure, but likely only weakly so. Please see our response to previous comment 2.

22) *Affirmation lines 33-34 is true on an annual basis but could be false during the monsoon season when subtropical warm depleted open ocean waters invade the shelf in the southern part of the Canary Upwelling System.*

As our focus is on the annual-mean nitrogen transport we keep this statement.

23) *L16-20, page 32: I agree that the western section is much more extended than the northern and southern exits but the role played by the West Africa Boundary Current (Mauritania Current here) plays a quite important role in cross-shore exchanges, it should be taken into account.*

We answered a similar comment made by Reviewer #1 (please see response to comment 25 by the first referee).

24) *L16-19, page 33: The final conclusion states that this study emphasizes the need for improving the resolution of eastern boundary currents in global coarse resolution models. I think it would be fair to cite at least Large and Danabasoglu (2006) who stressed this point 15 years ago.*

We now cite Large and Danabasoglu (2006) as a previous study pointing towards a similar conclusion (please see lines 24-25, page 27).

A Lagrangian study of the contribution of the Canary coastal upwelling to the open North Atlantic nitrogen budget

Derara Hailegeorgis[1], Zouhair Lachkar[1], Christoph Rieper[2,3], and Nicolas Gruber[2]

[1]Center for Prototype Climate Modeling, New York University Abu Dhabi, Abu Dhabi, UAE

[2]Environmental Physics, Institute of Biogeochemistry and Pollutant Dynamics, ETH Zurich, Universitätstrasse 16, 8092 Zurich, Switzerland

[3]Experimental Oceanography, Institute of Oceanography, University of Hamburg, Bundesstrasse 53, 20146 Hamburg, Germany

Correspondence: Zouhair Lachkar (zouhair.lachkar@nyu.edu)

Abstract.

The Canary Current System (CanCS) is a major Eastern Boundary Upwelling System (EBUS), known for its high nearshore productivity and for sustaining ~~large fisheries. Only a part of the inorganic nutrients that upwell along Northwest Africa are being used to fuel the high nearshore productivity. The remainder together with some of the newly formed organic nutrients are exported offshore into~~ a large fishery. It is also an important, but not well quantified, source of nitrogen to the adjacent oligotrophic subtropical gyre of the North Atlantic. ~~Yet, the offshore reach of these nutrients and their importance for the biogeochemistry of the open North Atlantic is not yet fully quantified.~~ Here, we ~~determine the lateral transport of both organic and inorganic nitrogen from the Canary upwelling and investigate the~~ use a Lagrangian modelling approach to quantify this offshore transport and investigate its timescales, reach, and ~~structure of offshore transport using a Lagrangian modelling approach. To this end, we track all water parcels entering the coastal ocean and upwelling along the Northwest African~~ contribution to the fueling of productivity in the offshore regions. In our Lagrangian model, we release nearly 10 million particles off the Northwest African coast and then track all those that enter the nearshore region and upwell along the coast between 14°N and 35°N~~, as simulated by~~ . We then follow them as they are transported offshore, also tracking the biogeochemical transformations, permitting us to construct biogeochemical budgets along the offshore moving particles. The three-dimensional velocity field as well as the biogeochemical tracers and fluxes are taken from an eddy-resolving configuration of the Regional Ocean Modeling System (ROMS). Our ~~model analysis suggests that the vast majority of the upwelled waters originate from offshore and below the euphotic zone (70 m depth), and once upwelled remain in the top 100m. The offshore transport is intense, yet it~~ Lagrangian model analysis reveals a very intense offshore transport of nitrogen, with about 20-40% in the form of organic nitrogen. The transport varies greatly along the coast. ~~The~~ Even though the central CanCS (21°N-28°N) transports the largest amount of water offshore, ~~thanks to a larger upwelling volume and a faster offshore transport . In contrast,~~ its offshore transport of nitrogen is somewhat smaller than that in the southern CanCS (14°N-21°N)~~exports more nitrogen from the nearshore~~, primarily because of the higher nitrogen-content of ~~its upwelling waters . Beyond 200 km, this nitrogen offshore transport declines rapidly because the shallow depth of most water parcels supports high organic matter formation and subsequent export of the organic nitrogen to depth. The horizontal pattern of offshore transport is characterized~~

~~by latitudinally alternating offshore-onshore corridors indicating a strong contribution of mesoscale eddies and filaments to the mean transport~~the upwelling waters there. Around 1/3 of the total offshore transport of water occurs around major capes along the CanCS. The persistent filaments associated with these capes are responsible for an up to four-fold enhancement of the offshore transport of water and nitrogen in the first 400km. Much of this water and nitrogen stems from upwelling at quite some distance from the capes, confirming the capes' role in collecting water from along the coast. North of Cape Blanc and within the first 500 km from the coast, water recirculation is a dominant feature of offshore transport. This process, likely associated with mesoscale eddies, tends to reduce the efficiency of offshore transport. ~~This process is less important in the southern CanCS along the Mauritanian coast.~~ The Canary upwelling is modelled to supply around 44 mmol N $m^{-2}yr^{-1}$ and 7 mmol N $m^{-2}yr^{-1}$ to the North Atlantic Tropical Gyral (NATR) and the North Atlantic Subtropical Gyral East (NASE) Longhurst provinces, respectively. In the NATR, this represents nearly half (~~45~~53±~~15~~26%) of the estimated total new production, while in the NASE, this fraction is small (~~3.5~~4±~~1.5~~2%). Our results highlight the importance of the CanCS upwelling as a key source of ~~nutrient~~ nitrogen to the open North Atlantic and stress the need for improving the representation of EBUS in global coarse resolution models.

1 Introduction

Over the last three decades, several studies have highlighted the importance of the coastal ocean in the global carbon cycle (e.g., Walsh 1991; Wollast, 1998). For instance, it has been estimated that continental margins contribute nearly half of the globally integrated oceanic primary production, although they only occupy about 10% of the world ocean surface (Walsh, 1991; Smith and Hollibaugh, 1993; Muller-Karger et al., 2005; Liu et al., 2010; Jahnke, 1990). The coastal ocean is not only highly productive, but is also a major source of nutrients and organic matter to the open ocean (Liu et al., 2000, 2010; Lovecchio et al., 2017; Frischknecht et al, 2018). For example, Wollast (1998) and Ducklow and McCallister (2004) estimated that about half of the total production in the coastal ocean is exported laterally~~, leading to substantial modifications of the biogeochemical cycles there~~. Globally, the magnitude of this lateral export of organic and inorganic matter from the coastal ocean into the open ocean is ~~ill constrained~~ ill-constrained and highly debated. Additionally, little is known about the exact fate and impact of this laterally exported matter in the open ocean. It is generally assumed that most of the organic matter eventually gets remineralized back to its inorganic constituents. In extreme cases, the associated increase in heterotrophic activity may actually exceed the amount of autotrophic production, making such systems net heterotrophic. Potential places for this to occur are the subtropical gyres where strong nutrient limitations ~~leads~~ lead to low levels of productivity (Del Giorgio et al., 1997; Duarte and Agusti, 1998). The coastal ocean represents also ~~a potentially~~ an important, although not well understood, conduit in the global carbon and nutrient cycles. ~~Especially low-latitude upwelling margins could play a crucial role in the~~ Upwelling margins serve as a return pathway of carbon and nutrients from the deep ocean, where they accumulate due to sinking, back to the ~~low-latitude surface ocean, which is needed in order to compensate for the continuous loss of these elements from the low latitude ocean through sinking into the deep ocean~~ surface ocean. This is especially true in the low latitudes , (Gruber and Sarmiento, 2002).

Yet, despite decades of research, our ability to constrain this conduit in a quantitative manner has remained very limited (cf. Holzer and Primeau, 2008).

The Eastern Boundary Upwelling Systems (EBUS) play a particularly important role for the global exchange of organic and inorganic matter between the coastal and open oceans. These systems are among the most productive ecosystems in the world and sustain a high fraction of global export production and global fish catch (Pauly and Christensen, 1995; Carr, 2001; Hansell, 2002; Chavez and Messie, 2009). Their productivity is fuelled by nutrient-rich water that upwells at the coast due to alongshore equatorward winds. Although the four major EBUS in the world make up a small part of the global ocean (0.1% - 0.3% in most studies), they account for 30% of the world's fish catch (Durand et al. 1998; Carr and Kearns, 2003; Rykaczewski and Checkley, 2008; Arístegui et al. 2009). The lateral transport of inorganic and organic matter is potentially particularly relevant for EBUS, as they export this material into the adjacent subtropical gyres. These gyres are likely particularly receptive as they have low nutrient conditions (oligotrophic) and have been shown to be net heterotrophic based on observational data (Duarte and Agustí, 1998; Del Giorgio and Duarte, 2002). Yet, the question of whether and how far into the open ocean the additional input of organic and inorganic matter can increase in situ respiration and new production (NP) remains a subject of a long and unresolved debate (Smith and Hollibaugh, 1993; Duarte and Agustí, 1998; Liu et al., 2010; Lovecchio et al., 2017).

Located along the northwestern African coast, the Canary Current System (CanCS) constitutes the EBUS of the North Atlantic subtropical gyre (Pelegri et al., 2005a; Pelegri et al., 2006; Barton, 1989). The CanCS is composed of the Canary Current (CC) and the Canary Upwelling Current (CUC). The CC represents the eastern boundary current of the North Atlantic Subtropical Gyre. It flows parallel to the Moroccan coast and merges with the westward North Equatorial Current (NEC) around Cape Blanc (21°N) (Barton, 1987; Hernandez-Guerra et al., 2005). The CUC is a nearshore surface jet associated with the upwelling flowing coastal upwelling front, which flows equatorward along the northwest African coast (Pelegri et al., 2006). The Cape Verde frontal zone, between Cape Blanc and the Cape Verde archipelago, is dominated by a permanent cyclonic circulation with a poleward boundary current, the Mauritanian current (MC), that extends at depth beyond Cape Blanc as a slope undercurrent typical of eastern boundary upwelling systems (Barton et al., 1989; Arístegui et al., 2009). Upwelling is permanent along most of the Moroccan coast (21-35°N), albeit with weaker intensity and stronger seasonality north of 26°N (Cropper et al., 2014). South of Cape Blanc, upwelling is present essentially in late fall and winter (October-March). Upwelled waters have different nutrient contents depending on their respective sources. North of Cape Blanc, the relatively nutrient-impoverished North Atlantic Central Waters (NACW) feed most of the upwelling (Mason et al., 2012). In contrast, waters upwelling south of Cape Blanc have a higher nutrient content as they are fed by the nutrient-richer South Atlantic Central Waters (SACW) brought by the MC (Schutte et al., 2016; Kounta et al., 2018; Glessmer et al., 2009; Peña-Izquierdo et al., 2015).

Intense mesoscale structures, including eddies and filaments develop in different parts of the CanCS and contribute to the offshore transport of the coastal waters (Lovecchio et al., 2018). Àlvarez-Salgado et al. (2007) estimate that persistent coastal filaments at the West African coast and Iberia export carbon at a rate 2.5 - 4.5 times higher than Ekman transport. Pelegri et al. (2005a) found that in the Canary Basin coastal filaments and cyclonic eddies cause localized offshore export of nutrients and organic carbon. The role of upwelling filaments in the shelf to open ocean transport of organic matter depends also on eddy-filament interactions, which frequently occur on ocean margins (e.g. Barton et al., 1998; Brink and Cowles, 1991). Oceanic eddies may entrain filament waters with higher content of organic matter, enhancing the shelf-ocean exchange (Aristegui et al., 1997). Filaments may return to the continental shelf part of the water upwelled and expelled from the coast by means of eddy-associated circulation. This recirculation decreases the impact of filaments on the offshore transport of organic matter (e.g. Basterretxea and Aristegui, 2000).

The quantification of the magnitude and type of lateral export is challenging due to the complex biogeochemical and physical dynamics of the offshore transport. Much of it is being driven by mesoscale processes, whose appropriate in-situ sampling goes beyond the abilities of current observing systems, thus requiring the use of high-resolution coupled physical/biogeochemical models. Yet, the number of high-resolution model-based studies that addressed and quantified the coastal-open ocean exchange in the CanCS remain limited (e.g., Fischer and Karakas, 2009; Lachkar and Gruber, 2011; Pastor et al., 2013; Auger et al., 2016; Lovecchio et al., 2017; Lovecchio et al., 2018). Such studies have stressed the importance of eddies and coastal filaments in the offshore transport of coastal upwelling. Lovecchio et al. (2017), for example, examined the export of organic carbon from the CanCS using a coupled physical-biogeochemical ocean model with a telescopic grid that covers the whole Atlantic ocean while maintaining a high resolution along the coast of northwest Africa. They demonstrated that about a third of the organic carbon produced along the northwest African coast is transported offshore, and some of it well beyond 1500 km from the coast, contributing substantially to the net community production there. In a follow-up study, Lovecchio et al. (2018) showed that much of this transport is driven first by filaments (in the first 100 km from the coast), and then later taken over by westward propagating mesoscale eddies. However, these authors focused on the transport of organic carbon only ~~, and therefore~~ and so did not estimate the contribution of the Canary upwelling to the offshore export of nutrients into the open ocean and the implications this might have for the biogeochemistry of the North Atlantic Ocean. Furthermore, the Eulerian approach used by Lovecchio et al. (2017, 2018) does not allow for the identification of ~~the contribution of the upwelled waters . It is also not well suited for the identification and quantification of the pathways of~~ waters that upwell at the coast and the ~~coastal-open oceanexchange~~tracking of their trajectories after they enter the open ocean.

Here, we aim to close this gap, and investigate the contribution of the upwelling waters to the nitrogen budget of the open North Atlantic, thereby considering the transport of both organic and inorganic forms of nitrogen. To this end, we use a Lagrangian approach to quantify the offshore reach, the spatial structure and the dominant timescales of the offshore transport of upwelled waters by tracking all open ocean waters that upwell along the coastal region of the CanCS. Lagrangian approaches have a long and rich history in the study of dynamical systems, especially in the atmosphere (Lin et al., 2012), but also in the ocean (van Sebille et al., 2018), as they present a number of advantages relative to the much more commonly used Eulerian approach, especially in the context of offshore transport., By taking the moving particle as a frame of reference, the Lagrangian tracking of water masses is much better suited to analyze the connectivity between the coastal and the open ocean regions. Furthermore, the Lagrangian method can be used to derive conditional statistics where subsets of particles that fulfill certain criteria are analyzed. This is useful for instance here to restrict the analysis of offshore transport to upwelling particles only. By not only tracking waters through the appropriate seeding of Lagrangian particles, but also tabulating the biogeochemical transformations along the pathways, we can also establish Lagrangian budgets. This permits us to develop a holistic perspective of the pathways taken by nutrients and carbon along their journey from the ocean's interior through upwelling and then their offshore transport to their ultimate fate of being exported to depth again (Frischknecht et al., 2018). Such an analysis of the origin, transformation and fate is impossible to undertake when using an Eulerian point of view. Thus, our Lagrangian approach permits us to take deep insights into the working of the CanCS system and its connection to the open ocean.

Previous studies have used the Lagrangian approach to study different aspects of the CanCS. For instance, Brochier et al. (2011) conducted a ROMS-based Lagrangian experiment to study the transport of ichthyoplankton (fish eggs and larvae) due to filaments between the West African coast and the Canary Islands. Mason et al. (2012) used a Lagrangian approach to characterize the source waters of upwelling in the CanCS between 31°N and 35°N. Yet, these studies were limited to specific regions of the CanCS and did only partially sample coastal upwelling there. Here we substantially expand on these previous efforts by sampling and tracking all open ocean waters that upwell along the West African coast between 14°N and 35°N, and ~~quantify~~ quantifying the offshore export of water, nutrients and organic matter. We also investigate the kinetics and the structure of this offshore transport and explore the role of water recirculation and capes in enhancing both coastal upwelling and offshore export. Finally, we examine the contribution of the CanCS upwelling to the Open North Atlantic nitrogen budget.

2 Methods

2.1 ~~Model setup~~Models and configuration

2.1.1 ~~Models and configuration~~

We use a CanCS configuration of the Regional Ocean Modeling System (ROMS)-AGRIF (http://www.croco-ocean.org/) similar to that used by Lachkar et al. (2016). ROMS solves the primitive equations and has a free-surface and a terrain-following vertical coordinates (Shchepetkin and McWilliams, 2005). We use a rotated-split third-order upstream biased operator for the advection of momentum and material properties (Marchesiello et al., 2009). The non-local K-profile parameterization (KPP) scheme is used to represent the subgrid vertical mixing (Large et al., 1994). The biogeochemical model is a nutrient-phytoplankton-zooplankton-detritus (NPZD) model based on nitrogen (Gruber et al., 2006). It uses a system of ordinary differential equations representing the time-evolution of the following state variables: nitrate (NO_3^-), ammonium (NH_4^+), phytoplankton, zooplankton, two pools of detritus and a dynamic chlorophyll-to-carbon ratio. The two classes of detritus represent, respectively, fast-sinking large organic matter particles and slow-sinking small particles. The small particles can coagulate with phytoplankton to form large detritus. In the water column, small and large detritus are remineralized to ammonium at rates of 0.03 and 0.01 day^{-1}, respectively. Sinking particulate organic matter that reaches the seafloor is also remineralized to ammonium at a rate of 0.003 day^{-1} (Gruber et al., 2006).

The model domain covers the region from 10°N to 42°N in latitude and from 30°W to 6°W in longitude with a grid resolution of 1/20°. This corresponds to a mesh size of about 5 km, which is sufficient for fully resolving mesoscale processes. The vertical grid consists of 32 layers with enhanced resolution near the surface. The bathymetry is derived from the ETOPO2 file provided by the National Geophysical Data Center (Smith and Sandwell, 1997) and a minimum bathymetry of 50is set.

We use a monthly climatological forcing based on the Comprehensive Ocean, Atmosphere Data Set (COADS) (da Silva et al., 1994) for surface heat and freshwater fluxes. Surface temperature and salinity are restored to COADS observations using kinematic heat and freshwater flux corrections following Barnier et al. (1995). Wind stress is derived from the QuikSCAT-based Scatterometer Climatology of Ocean Winds (Risien and Chelton, 2008). The initial and lateral boundary conditions for temperature, salinity and nitrate are derived from the World Ocean Atlas (WOA) 2009. Other ecological tracers are initialized uniformly to arbitrary low values. Currents at the boundaries are derived from temperature and salinity data using geostrophy together with Ekman transport in the upper 40 m. The model starts from rest and is spun up for 12 9 years. We use the last then run it for 3 years of the simulation (i.e., Year 10 to Year 12) for analysis. Model outputs are stored at more years, on which we carry out the analysis, and store these outputs at a daily frequency.

2.1.1 Model evaluation

Surface (a-b) currents (in m s^{-1}) and (c-d) eddy kinetic energy (in cm^2 s^{-2}) as simulated in the model (left) and from surface drifter climatology of Lumpkin and Johnson (2013) (right). (a-b) Arrows indicate the direction of the current and the color shading shows the current magnitude.

Sea surface (a-b) temperature (in °C) and (c-d) chlorophyll-a concentrations (in mg m^{-3}) as simulated in ROMS (left) and from AVHRR and SeaWiFS data (right). The AVHRR and the SeaWiFS climatologies are computed over the periods from 1981 to 2016 and from 1997 to 2009, respectively.

Taylor diagrams describing statistical comparisons of modeled and observed (a) annual mean and (b) seasonal anomaly estimates of sea surface temperature (orange), salinity (pink), NO_3^- (blue) and chlorophyll-a (green) in the 0-100 km nearshore region (data points labeled “1”), the 100-500 km offshore region (data points labeled “2”) and across the entire model domain (data points labeled “3”). The reference point of the Taylor diagram corresponds to SeaWiFS observations for chlorophyll, AVHRR data for sea surface temperature, world ocean database (WOD) 2013 for surface salinity and nitrate.

The model successfully simulates the Canary current flowing parallel to the Moroccan shore and its detachment from the coast and merger with the westward NEC around the latitude of Cape Blanc (Fig. 1). However, the strength of both the northward coastal Mauritanian current in the south (16-20°N) and the eastward Azores current in the north (34°N) is underestimated in the model in comparison to the drifter data. The model simulates successfully the surface Eddy kinetic energy (EKE, Fig. 1) in the central and southern subregions as it reproduces quite accurately the high-EKE values observed downstream the Canary islands and the Cape Verde Archipelago and around the Cape Verde Peninsula in Senegal (Fig. 1). However, the model tends to underestimate EKE associated with the Azores current in the northern part of the domain. This might be due to the too weak Azores current in our model as well as the lack of high-frequency variability in the employed (climatological) forcing.

Despite a large-scale cold bias of around 1°C throughout most of the domain, the model captures the main patterns of the observed sea-surface temperature (SST) from the Advanced Very High Resolution Radiometer (AVHRR) satellite data (Fig. 2). In particular, the model reproduces the observed offshore gradient in SST, as well as the offshore extent of the cold upwelling region. The model simulates the spatial pattern of the observed chlorophyll-a (SeaWiFS, Fig 2) reasonably well over much of the domain, with high-concentrations in the upwelling region and lower concentrations in the open oligotrophic ocean (Fig. 2). The north-south chlorophyll gradient is also well reproduced with the southern part of the Canary system being more productive than the northern part. However, the model underestimates the observed cholorophyll-a in the nearshore regions, particularly in the southern part of the domain.

A more quantitative evaluation of the model skill can be achieved using both satellite data and in situ observations from the World Ocean Database 2018 (WOD 2018). We binned the latter onto a 0.5° monthly climatology without any spatial interpolation. This permits us to compare the model and observations only in those grid points where observations are available. The results of this evaluation are summarized graphically using Taylor diagrams (Taylor, 2001) quantifying the similarity between the observations and model in terms of their correlation, the amplitude of their standard deviations and their centered root mean square difference (rmsd) (Fig. 3The model was evaluated by confronting its outputs to a wide array of in-situ and satellite-based observations (see supplementary material section for full details). We find that the simulated and observed mean SST have similar standard deviations and correlate very strongly with correlation coefficients above 0.95 for both nearshore and offshore regions (Fig. 3a). Similarly, the quantitative comparison of the simulated and observed sea surface salinity (SSS) shows similar standard deviations and a small rmsd, as well as very high correlations ($r > 0.9$) in the nearshore and throughout the domain. Mean surface nitrate in the model has a comparable variance but a weaker correlation ($r \approx 0.7$) with observations. Simulated mean surface chlorophyll-a is moderately ($0.6 < r < 0.8$) correlated with observations and displays a substantially weaker variance than the satellite data.

The seasonal anomaly of SST in the model agrees well with observations at all distances from the coast with both the correlation coefficient and normalized standard deviation being over 0.9 (Figure 3b). SSS seasonal anomalies in the model correlate less strongly with observations with both correlation coefficients and normalized standard deviations having values below 0.7. Simulated surface nitrate seasonal anomalies show very similar variance in comparison to observations but correlate only weakly with data ($0.3 < r < 0.5$). The simulated surface chlorophyll-a seasonal anomalies have a similarly weak correlation with the observations in addition to a lower normalized standard deviation (below 0.5).

We finally evaluate the model ability to reproduce the three-dimensional distributions of temperature, salinity and nitrate in the upper ocean (Figure 2 in Supplementary Information (SI)). At all depth ranges (top 100 m, top 400 m and top 1000 m), mean temperature, salinity and nitrate are all reproduced quite well with correlations above 0.9 and normalized standard deviations near 1. The seasonal anomalies (shown only for the depth range of 0 - 400 m), are less accurately captured by the model. Temperature anomaly in the top 400 m is captured relatively well with a correlation close to 0.8 and a standard deviation comparable to observations. Salinity and nitrate anomalies show lower correlations (0.3-0.4), diverge further in rmsd (close to 1) and have a narrower distribution with a standard deviation of around 0.6.

In summary, despite some local biases and discrepancies with observations, the model generally shows good skill in reproducing the large-scale features of the circulation and the productivity of the Canary current region (Figs S1, S2). More importantly, it reproduces well the strength and structure of the Canary coastal upwelling and captures the observed vertical structure of nitrate and organic matter (Figs S3 to S17). Overall, this CanCS-only ROMS setup has similar strengths and weaknesses as the telescopic grid setup employed by Lovecchio et al. (2017, 2018). We will discuss the potential impact of the model limitations on our results in the discussion section.

2.2 Lagrangian experiment

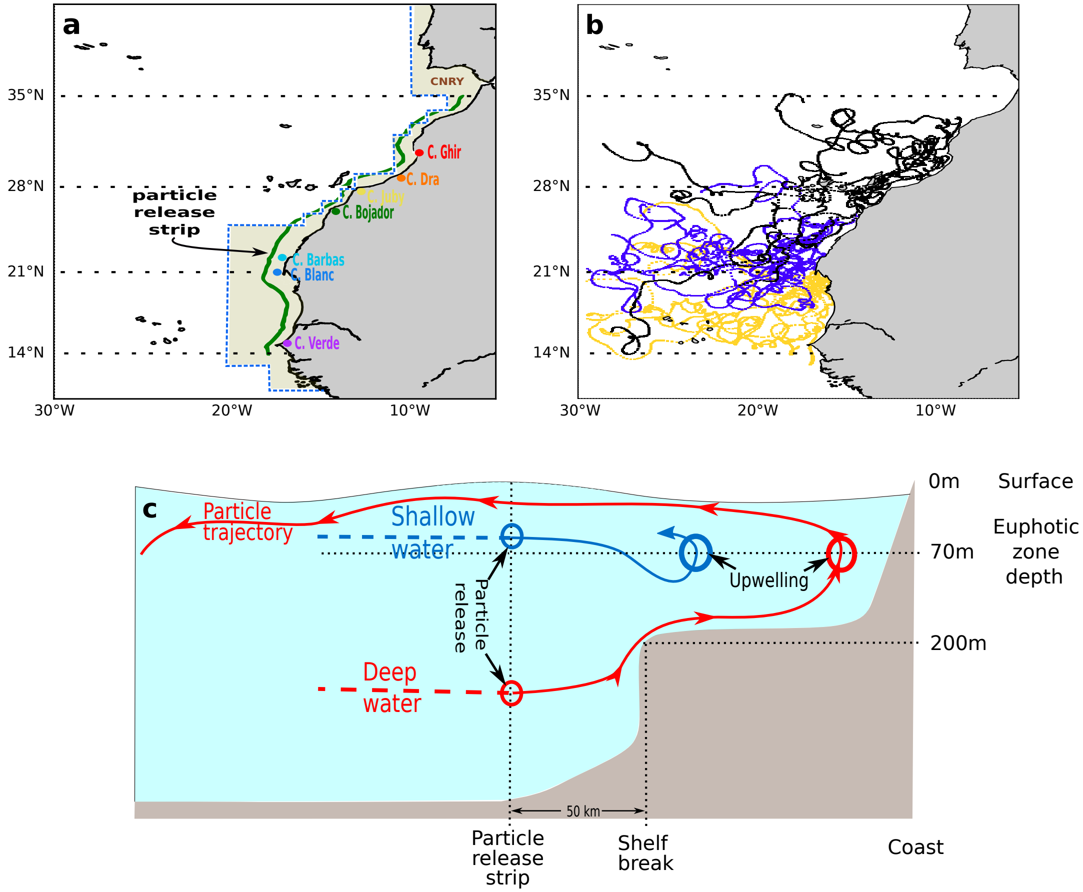

Figure 1. (a) The model domain stretches from 30°W to 6°W and from 10°N to 41°N. The solid green line indicates the limit of the coastal strip where particles are released at each vertical layer proportionally with the onshore water volume transport. The black dotted lines partition the domain into the three latitudinal subregions: the southern CanCS (14°N - 21°N), the central CanCS (21°N - 28°N) and the northern CanCS (28°N - 35°N). The yellow shaded area corresponds to the portion of the Longhurst Canary Coastal Province (CNRY) that lies within the model domain. The location of the seven capes studied in Section ~~4.1~~ 5.1 is shown here in ~~different~~ different colors. (b) A plot of sample trajectories of 10 randomly selected particles in our Lagrangian experiment from each of the southern (golden), central (blue) and northern (black) subregions. (c) A schematic of the Lagrangian sampling of upwelling particles. Particles are released when open ocean water enters the coastal strip. Based on their depth when released, we term particles to be of shallow (< 70 m) or deep (> 70 m) source. Since their release into the coastal region, particles are marked as upwelling the first time they cross the 70 m depth and their trajectory tracked thereafter.

The Lagrangian particle tracking experiment is performed offline with ARIANE (Blanke and Raynaud, 1997; http://stockage.univ-brest.fr/ grima/Ariane/) using ROMS daily output. ARIANE tracks water particles based on the velocity output of the model. In this experiment, ARIANE runs based on the model output of zonal and meridional velocities (ARIANE internally computes vertical velocities from the continuity equation). ARIANE analytically computes streamlines of particle trajectories across grid-walls by assuming a steady-state flow. The data points for successive days are used as piecewise steady flow where the experiment velocity is assumed to be static for each day and not interpolated between different days. The velocity at a given point inside the regular cells of the model is computed by linearly interpolating the velocity at opposite faces of a cell. ARIANE's computation of particle trajectories doesn't account for the subgrid vertical mixing in the model.

With our Lagrangian experiment we aim to study trajectories of open ocean water masses that enter the coastal region and upwell between 14°N and 35°N (see sample trajectories in Figure 1b). This region extends in north-south direction a total of 3185 km and covers most of the West African coast component of the Canary Current Coastal Province (CNRY) of Longhurst et al. (2007) (Fig. 4a, Fig 3 in SI). The control box 1a, Fig S20). To this end, we carry out our Lagrangian experiment in three steps: particle release (quantitative ARIANE experiment), particle tracking (qualitative ARIANE experiment) and upwelling identification (see the schematic in Fig S18).

In the quantitative experiment, a coastal upwelling region is set up between 14°N and 35°N. This region is bounded by the particle release strip (both entry and exit) to the west, the coast to the east and particle exit (but not entry) sections at the northern and southern ends of the upwelling coastal region (Figure 4a). Since particles are released only along the western segment of the control box, only open ocean particles that enter the coastal region are tracked and considered candidates for upwelling. The 1a). The particle release strip is set at the limit of the continental shelf defined at 50 km westward of the 200 m isobath along the coastindicating the limit of the continental shelf is identified and particles are released up to 50 km further west from it (Fig. 4b). This , which ensures sampling coastal upwelling occurring at the shelf break (Fig. 1b). This results in a coastal strip upwelling region with a width that varies from below 60 km near 27°N where the the continental shelf is narrowest to over 160 km near 25°N where the shelf is widest. Particles are released on a daily basis during one year and their trajectories are tracked during a two-year period. Particle release is based on the onshore water flow volume into the coastal region, where each particle is tagged with the corresponding initial transport. We limit the maximum transport a particle is associated with to 0.01 Sv, which limits the maximum volume assigned to one particle to 0.864 km^3. In total Through a daily particle release for one year at each cell along the particle release strip, a total of 9,888,387 particles are releasedover the first year (the period of particle release). By the end of the quantitative experiment, for each particle, we have its location, time of release and associated water volume.

A qualitative ARIANE experiment is then run on the initial conditions set by the quantitative experiment to track the particle trajectories and their along-path nitrogen concentrations. Particles are tracked for 720 days since their release until they leave the simulation's domain. Along each particle's trajectory, its latitude, longitude and depth are recorded saved daily along with biogeochemical tracersand the water volume tagged with each particle at its release that is assumed to follow the particle throughout its trajectory. Note that around 4.2%, 0.37% and 0% of the particles released in the southern, central and northern subregions, respectively, leave the domain southward or northward within one year of their release. Assuming the ocean to be an incompressible fluid and its velocity field to be non-divergent, the volume transport is conserved. ~~This allows ARIANE to compute particle trajectories and volume transports both forward and backward in time.~~ We quantify the amount of nutrients carried by each particle to a given location as the product of its associated volume and the concentration of the tracer associated with the particle when it reaches that location. ~~Tracked~~

Subsequently, tracked particles that enter the coastal region and cross upwards the 70 m depth~~to move up to shallower depths~~, the average depth of the euphotic zone in the Canary coastal region, are identified as ~~upwelling~~ upwelled particles. Since only particles that enter the coastal area and upwell there are followed, our experiment disregards wind stress curl-driven upwelling that occurs in the open ocean and can locally be important, particularly in the southern subregion (Lovecchio et al., 2017). From all tracked particles, 352,873 (3.57%) upwell~~. These are the particles that we follow thereafter and~~, which form the basis for our analyses (see additional details ~~of the Lagrangian experiment in SI~~in Fig S18).

Previous studies have shown subregional differences within the CanCS in circulation patterns, mesoscale activity, seasonality of upwelling, biology and sub-surface nutrient concentration (Arístegui et al., 2009; Pelegri and Benazzouz, 2015; Lovecchio et al., 2017). We thus separately characterize the trajectories of waters that upwell in three latitudinal subregions of the upwelling domain. These subregions cover southern (14°N - 21°N), central (21°N - 28°N) and northern (28°N - 35°N) parts of the CanCS (Figure ~~4a~~1a).

3 Characteristics of upwelling

3.1 ~~Upwelling of water~~

Our Lagrangian analysis reveals an annual upwelling of offshore-derived waters of nearly 80,000 km^3 (see Table 1). This is about 25 km^3 of water per year per kilometer of coastline, or 0.8 m^3 s^{-1} per meter of coastline. The strongest upwelling occurs in the central CanCS, with a particularly strong peak around Cape Bojador (27°N) (Fig. ~~5a~~2a). This subregion alone is responsible for more than half of the total upwelling (40,705 km^3 yr^{-1}). The northern subregion contributes about 25,000 km^3 per year to the upwelling, while the southern subregion has the smallest upwelling (13,000 km^3 yr^{-1}).

	Particles (yr^{-1})	Water (km^3 yr^{-1})	N (Gmol yr^{-1})	Median dist (km)	To 400km (%)	To 1000km (%)
Southern	51,275	13,~~178.9~~ 179	~~337.7~~ 338	64.1	~~95.4~~ 95	~~77.8~~ 78
Central	162,304	40,~~704.8~~ 705	~~210.3~~ 210	37.1	~~92.5~~ 93	~~69.3~~ 69
Northern	139,294	25,~~038.0~~ 038	~~86.8~~ 87	41.1	~~71.7~~ 72	~~33.1~~ 33
Whole CanCS	352,873	78,~~921.7~~ 922	~~634.8~~ 635	~~42.9~~ 43	86.3	~~59.2~~ 59

Table 1. The annual number of upwelling particles and their associated water and nitrogen, the median distance of upwelling to the coast and the net transport of water to 400 km and 1000 km from coast (as percent of upwelling volume) in the three subregions as well as the entire CanCS region in our experiment.

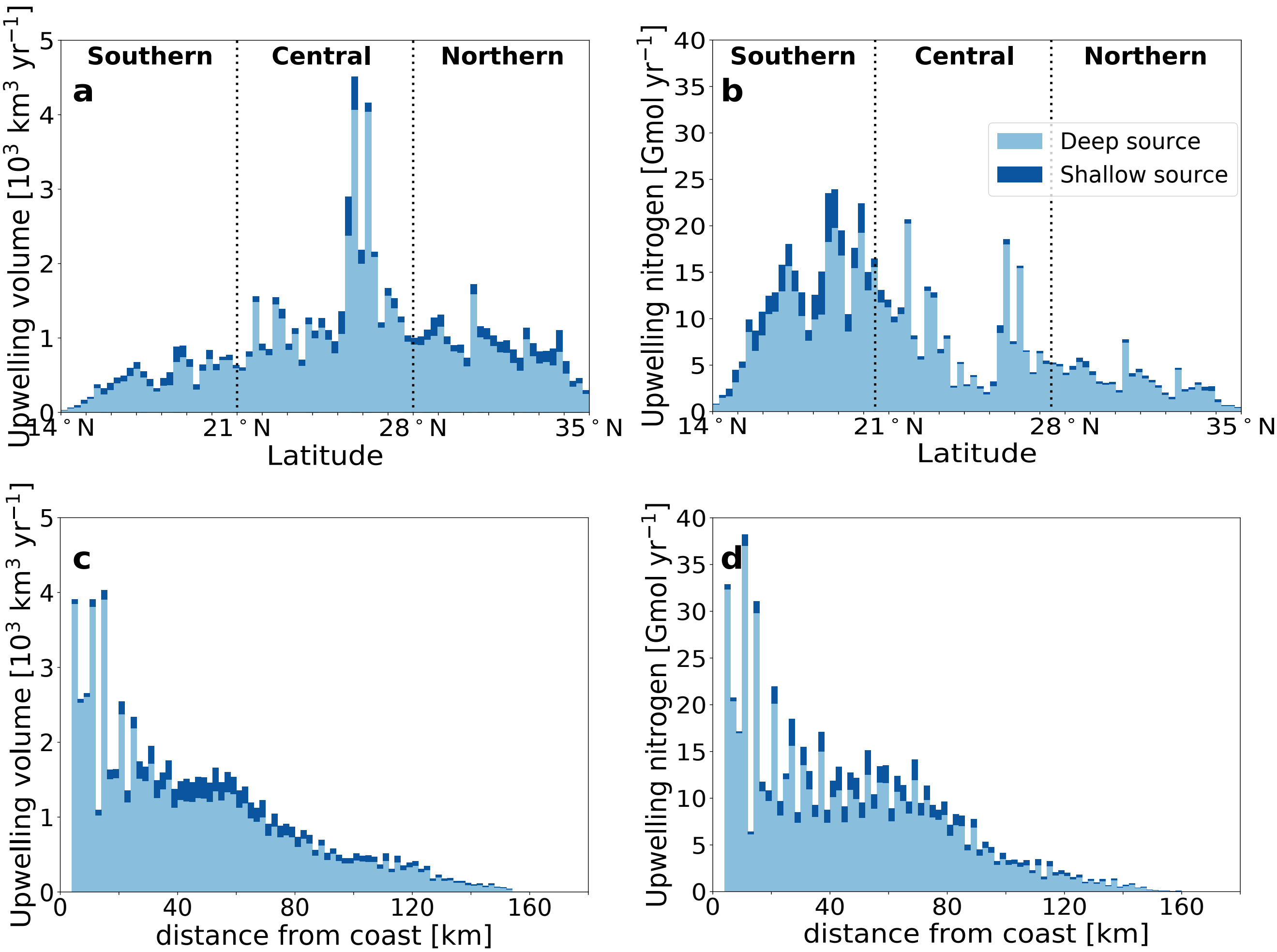

Figure 2. (a, b) ~~Zonally integrated annual~~ Annual upwelling (a) water volume ~~.~~ and (b~~,~~) nitrogen zonally integrated across the coastal upwelling region (between the coast and 50 km westward of the 200m bathymetry). (c,d) Annual upwelling (c) water volume and (d) nitrogen with distance from the coast in the whole CanCS upwelling domain (~~b) southern, (c) central and (d~~14°N-35°N)~~northern subregions~~. Light and dark blue segments represent contribution by deep and shallow sources of water, respectively.

Most of the upwelling stems from deeper waters, i.e., waters that enter our analysis region below 70 m. 85% of the tracked particles and 88% of the associated water volume follow that path (termed ’deep source’). The remaining upwelling stems from waters that enter the region within the euphotic zone and then are transported below 70 m before upwelling (here termed ’shallow source’) (Figure ~~4b~~1b). This fractional distribution varies little between subregions.

But the offshore distribution of the upwelling differs strongly between the three CanCS subregions (Fig ~~. 5). While the maximum of the upwelling in the Southern subregion occurs offshore at round 70 km distance from the shore with a weak onshore-offshore contrast, the central subregion has a clear maximum in upwelling in the first 20 km from the shore. The amount of upwelling then declines sharply with increasing offshore distance. The northern subregion has a first upwelling volume maximum right at the coast, followed by a second one at around 50 km from the shore. Beyond 80 km, there is hardly any upwelling.~~ S22). These differences are ~~well~~ reflected in the median upwelling distances being 64.1km, 37.1km and 41.1 km in the southern, central and northern subregions, respectively (Table 1).

Most of this variability has to do with the variability of offshore Ekman transport and curl-driven upwelling between the three subregions. For instance, the central subregion has strong year-round coastal upwelling whereas upwelling tends to be strong only in the summer season in the northern subregion (Pelegri and Benazzouz, 2015). Similarly, the Ekman-driven upwelling in the southern subregion is restricted to the winter and ~~late fall~~ spring (Pelegri and Benazzouz, 2015; Capet et al., 2017). There are distinct differences also with regard to the wind curl-driven upwelling between the three subregions. Indeed, the wind stress curl is predominantly downwelling-favorable in the northern and central subregions and upwelling-favorable in the southern subregion. This enhances upwelling in the southern region, particularly in the open ocean, but its effect is only partially sampled in the present study given our focus on the coastal region. Other inter-regional variations may also stem from the design of the experiment. For instance, our experiment ~~doesn’t identify coastal upwelling immediately~~ identifies limited coastal upwelling south of Cape Blanc and between Capes Barbas and Bojador because their bathymetry is shallower than the 70 m upwelling depth criterion used here. Furthermore, the upwelling strip is relatively narrow in the northern subregion because of the narrower shelf, thus limiting the offshore spread of coastal upwelling there (Figure ~~4 in SI~~S21).

3.1 ~~Upwelling of nitrogen~~

~~(a) Zonally integrated annual upwelling nitrogen. (b,c,d) Annual upwelling nitrogen with distance from the coast in the (b) southern, (c) central and (d) northern subregions. Light and dark blue segments represent contribution by deep and shallow sources of water parcels, respectively.~~

~~The~~ Finally, the upwelling patterns of water and nitrogen have a few important differences. The southern subregion has the lowest upwelling water volume yet the strongest upwelling flux of nitrogen (Fig. 2). This is primarily due to the shallower nutricline associated with a shallower thermocline there as well as the higher-nutrient content of the South Atlantic Central Waters (SACW) that feed upwelling south of Cape Blanc. ~~The central subregion has a moderate nitrogen flux associated with upwelling while~~ Conversely, the weakest upwelling-driven nitrogen flux is in the northern subregion ~~has the weakest upwelling flux of nitrogen~~ (Table 1, Fig. 2). ~~Finally, parcels that upwell further from the coast carry a nitrogen flux that is disproportionately lower than their corresponding associated water volume.~~

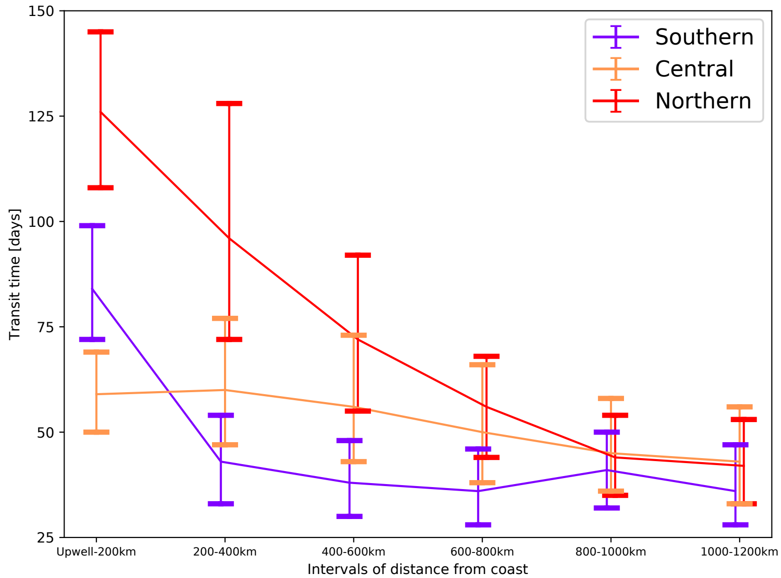

Figure 3. A plot of median transit times for particles to traverse subsequent intervals of distance from coast for the three subregions in the CanCS. The first point shows the transit time from particles' upwelling distances to reaching 200 km. The error bars indicate the 10 percentile distributions above and below the median transit times. Only particles that traverse the whole distance range are considered.

4 Offshore transport

4.1 Reach and timescales of offshore transport

Over the whole CanCS, the water offshore transit times (the median time for particles to traverse a given offshore distance interval) are longer in the nearshore region and decrease as we go further away from the coast (~~Table 2~~Fig 3). Large differences in the offshore transport timescales exist between the three CanCS subregions. In the first 200 km from the coast, the offshore transport is fastest for particles upwelled in the central subregion and slowest for those in the northern subregion (~~Table 2 and Fig. 5, SI~~Fig 3; Fig. S25). Indeed, in the central subregion, 80% of the upwelling particles reach 200 km in three months and 50% reach that distance in two months only. In contrast, less than 30% of particles upwelling in the northern subregion reach 200 km offshore in three months and it takes more than four months for half of them to reach that distance. At larger distances from the coast (beyond 400 km), the offshore transport becomes ~~faster~~ fastest for particles that upwelled in the southern subregion with nearly 80% of particles reaching 1200 km in two years, while only 70% and 30% of particles upwelling in the central and northern subregions, reach that distance in two years. This can also be seen in the water residence times being shortest ~~in~~ for the central subregion particles up to 400 km and ~~in~~ for the southern subregion particles beyond 400 km (Table ~~1, SI~~S1).

Upwell-200km 200-400km 400-600km 600-800km 800-1000km 1000-1200km Southern 84 43 38 36 41 36 Central 59 60 56 50 45 43 Northern 126 96 72 56 44 42 Whole CanCS 83 66 57 49 44 41 The median transit time (days) for particles to traverse each distance interval for the first time for the three subregions as well as the entire CanCS region in our experiment. The first column shows the transit time between upwelling and reaching 200 km offshore. Only particles that traverse the whole distance range are considered.

4.2 Net offshore transport

Integrated over the whole analysis domain from 10°N to 41.5°N, the CanCS exports over 70'000 $km^3\ yr^{-1}$ of water toward the open North Atlantic (Figure 7a4a). The maximum offshore transport is reached at close to 150 km from the shore at around the edge of the coastal upwelling area . The transport decreases thereafter most sampled upwelled water (nitrogen). It is around 150km because at closer distances to the coast (<100-150km), upwelled volume is only partially sampled, while further distances (>100-150km) are never reached by a proportion of particles because of recirculation retaining them close to the coast and alongshore transport exporting some particles out of the model domain. Beyond this maximum, the transport decreases gradually as the number of particles reaching farther offshore distances within the two-year integration period declines. But even at a distance of 1200 km from the coast, the offshore transport still amounts to 40'000 $km^3\ yr^{-1}$.

There are substantial differences between the different subregions. The central subregion of the Canary system is responsible for over half of the entire net offshore transport of water from the CanCS at any distance from the coast (Figure 7a4a). The offshore transport of associated with the northern subregion upwelling is initially very strong, but decreases sharply thereafter, so that beyond 800 km, it becomes the weakest of all three regions. This is because of its Reduced coastal upwelling and low offshore transport efficiency and the relatively low volume of upwelling (i.e., the ratio of offshore transport volume at a given distance to upwelling volume) explain this pattern (Table 1, Figure 7a4a). The southern subregion is associated with the smallest offshore transport of water up to 800 km offshore due to its small coastal upwelling volume.

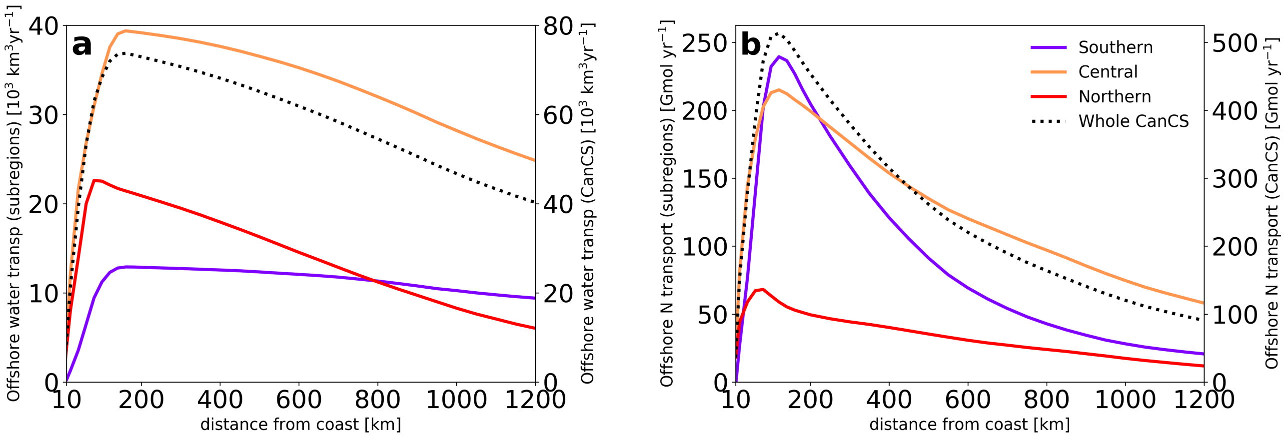

Figure 4. Net offshore transport of (a) water and (b) nitrogen as a function of the distance to the coast in the three subregions (left axis) as well as the entire CanCS (right axis) in our experiment.

~~At close to~~ Around 150 km from the coast~~(corresponding to the edge of the coastal upwelling stripe), the offshore transport of nitrogen reaches its maximum, reaching~~ , the nitrogen transport reaches values as large as 500 Gmol yr^{-1} ~~. Thereafter, the offshore transport decreases exponentially~~ at 200 km, decreasing exponentially further offshore, although with a relatively long decay length scale, such that at a distance of 1200 km, the offshore export of nitrogen still amounts to 100 Gmol yr^{-1}.

~~In spite of having the lowest offshore transport of water , the southern subregion exports the highest amount of nitrogen offshore at 200 km~~ Although offshore water transport was minimal for the southern CanCS particles, this subregion is responsible for the greatest offshore export of nitrogen (nearly half of the offshore export of nitrogen by the whole CanCS region at this distance). This is a direct consequence of the large upwelling flux of nitrogen (Table 1 and Fig. ~~7b). At larger distances from the coast, the situation reverses~~ 4b). This pattern reverses further offshore. Beyond 200 km from the coast, the offshore transport of nitrogen associated with the central subregion upwelling exceeds that originating from both the southern and northern subregions. At all distances ~~from coast~~ past 600km, the central subregion contributes over half of the nitrogen offshore export by the entire CanCS. At these distances, the nitrogen transport of waters stemming from the central subregion is at least twice as large as that from the southern subregion, and four times as large as that from the northern subregion.

The magnitude of the offshore transport of nitrogen at any distance from the coast depends both on the volume of offshore transport and how efficiently nitrogen is stripped from the waters by biological productivity and the resulting organic nitrogen exported to depth. It is thus instructive to assess the specific forms of nitrogen being transported offshore.

4.3 Nitrogen allocation

In the nearshore 50 km, phytoplankton is very efficient in taking up the inorganic nitrogen that is being upwelled, and fixing it into organic forms of nitrogen (Fig ~~8a~~5a). This results in nearly 100% of the offshore transported nitrogen to be in the form of organic nitrogen. But as additional nitrogen is being supplied from below, the fraction of the upwelled nitrogen that gets

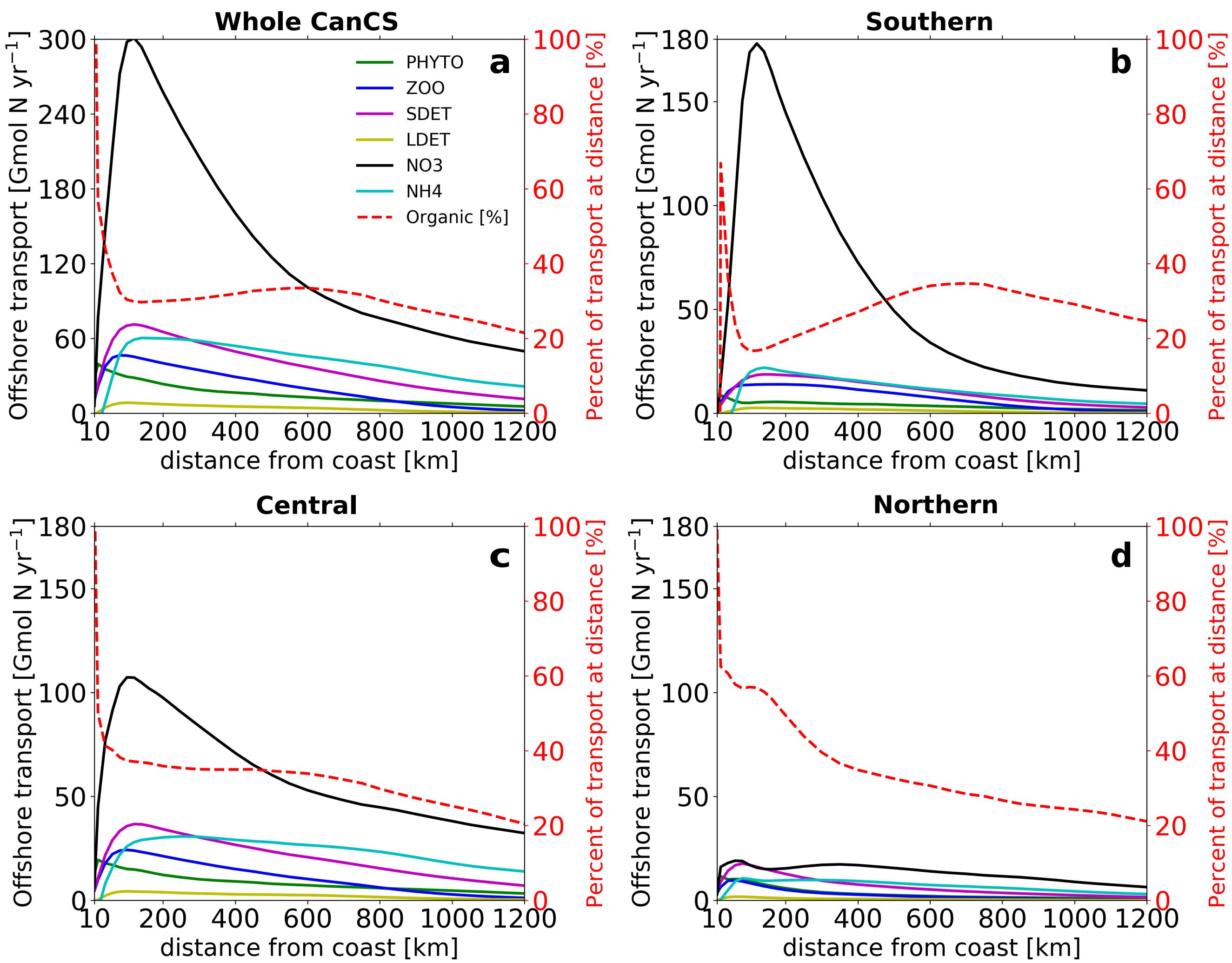

Figure 5. The net offshore transport of each pool of nitrogen (phytoplankton, zooplankton, small and large detritus, nitrate and ammonium) as a function of the distance to the coast in the three subregions (left axis). The fraction of organic nitrogen (in %) in the net offshore transport of nitrogen at each distance from the coast is shown on the right axis.

consumed decreases rapidly with increasing offshore distance. Furthermore, some of the fixed organic nitrogen is being lost through sinking, so that beyond the nearshore 50 km region, inorganic nitrogen in the form of nitrate dominates the nitrogen pool at all distances from the coast (Fig ~~8a~~5a). Beyond ~~200~~ 300 km, ammonia is the second largest pool. Overall, organic nitrogen contributes only 30% to the total nitrogen pool. Within the organic nitrogen pool, small detritus contributes the most to the offshore transport, while the contribution of phyto- and zooplankton is much smaller and that of the large detritus particles essentially negligible.

Given its dominance in terms of the total offshore transport, the southern subdomain is also the main region determining the whole CanCS pattern of nitrogen allocation (Fig ~~8b~~5b). In this southern subdomain, the fraction of organic nitrogen is particularly low, being only 20% at the peak of the offshore transport. With increasing distance, the fraction increases to 30%. This indicates a much further offshore extension of the conversion of inorganic nutrients to organic matter in this domain. The central domain has a nitrogen allocation pattern that is similar to that of the whole CanCS (Fig ~~8c~~5c), while the transport in the northern subdomain is not only weak, but also the least dominated by the offshore transport of nitrate (Fig ~~8d~~5d).

The different offshore gradients exhibited by the different pools of nitrogen can be largely explained by their position in the cycling of nitrogen within the euphotic zone and their susceptibility to sinking. Nitrate, being the dominant form of nitrogen being upwelled comes first, followed by phytoplankton, zooplankton, and small detritus. The latter two contribute then to the formation of ammonia by respiration and remineralization. Ammonia tends to accumulate, partially aided by its non-sinking nature, making this an important part of the offshore transport. In contrast, the very small contribution by the large detritus is largely a consequence of its rapid export to depth (see also Gruber et al., 2006).

4.4 ~~Depth structure~~ Structure of offshore transport

~~Upwelling~~

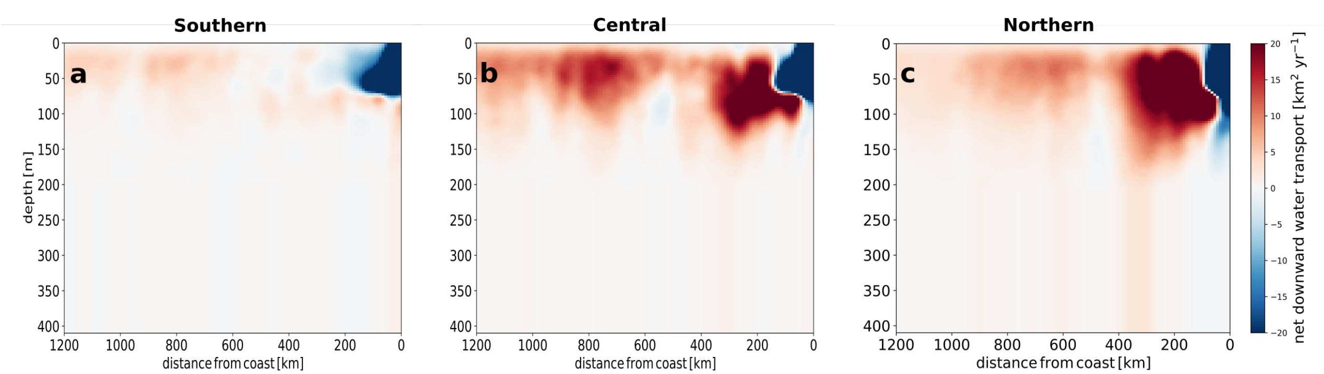

Figure 6. Meridionally integrated net downward transport of water in the (a) southern, (b) central and (c) northern subregions. All values are in km^3 of water per km of offshore distance per year.

Upwelled particles that are transported offshore are also subject to vertical circulation that distributes them vertically (~~Figs 7-8 in SI).~~ Fig 6, S27). Subduction may potentially slow down offshore transport since velocities deeper in the water column are smaller. However, subduction can also increase the efficiency of offshore transport by minimizing the depletion of nitrogen in surface waters.

For the northern and central subregions, upwelling particles are subject to moderate subduction at around 100 to 200 km from the coast (Fig ~~. 7, 8c, SI). This subduction is particularly strong in the upper 70 m and vanishes around 200 m.~~ 6). In the southern subregion, however, upwelling particles are subject to very little subduction while a strong ~~secondary upwelling in the open ocean~~ open ocean upwelling maintains them near the surface~~(Fig. 10 and Fig. 8c, SI). Indeed, the vast majority (>90%) of particles upwelling in the~~ . Similarly to the water volume transport, subduction of nitrogen is strongest in the northern subregion and weakest in the southern subregion ~~remain in the upper 100 m as they are transported offshore. In the central and northern subregions a smaller (>80%) but still important proportion of upwelling particles remain in the upper 100 m as they are exported offshore~~ (Fig. ~~9 and Fig. 8, SI~~S24). The stronger downward advective transport occurring in the central and northern subregions is due to a strong negative wind stress curl in these subregions, which is absent in the southern subregion (Lovecchio et al., 2017). Furthermore, persistent filaments associated with prominent capes in the central and northern subregions may contribute to enhanced subduction of upwelling water and nutrients there ~~. Similarly to the water volume transport, subduction of nitrogen is strongest in the northern subregion and weakest in the southern subregion (Fig. 10).For instance, at 400 km above 95% of nitrogen upwelled in the southern subregion remains in the top 100 m. This proportion drops to around 80% and 60% for the central and northern subregions, respectively (Fig. 9b~~(Lovecchio et al., 2018).

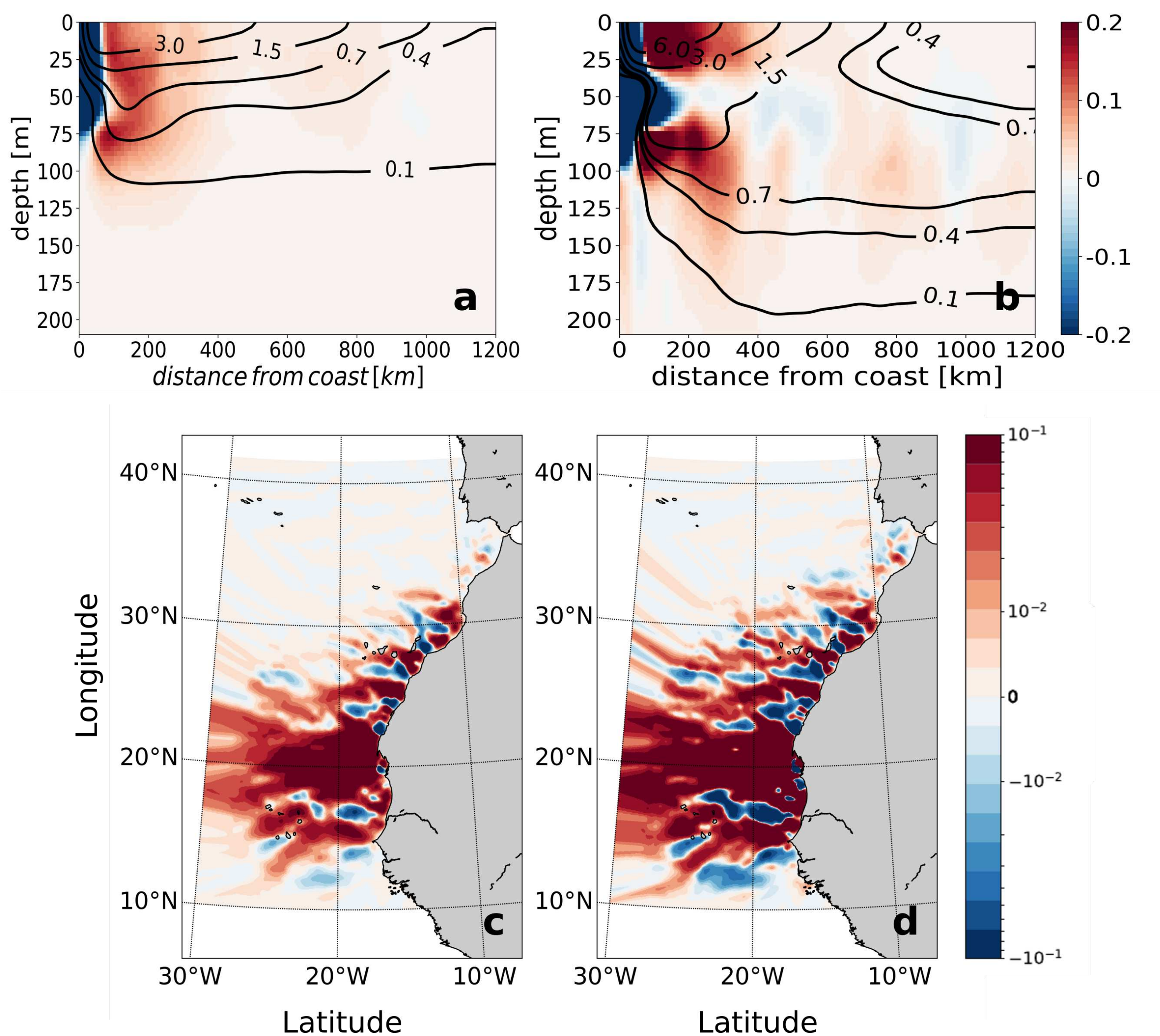

Figure 7. ~~Fraction~~ Analysis of the structure of the offshore transport of nitrogen: (~~in %~~a, b) Offshore sections of the meridionally integrated net downward and offshore transports of ~~upwelled~~ (a) ~~water~~ organic and (b) inorganic nitrogen ~~that remains above 100~~in the upper 200 m ~~at their first arrival~~ as a function of the distance to ~~each~~ the coast. Positive (red) and negative (blue) shadings represent net downward and net upward transports, respectively, (in Gmol N km^{-1} yr^{-1}) and contours correspond to the offshore ~~distance~~ transport (in Gmol N m^{-1} yr^{-1}). The fluxes were meridionally integrated throughout the ~~three subregions as well as~~ domain. (c, d) Maps of the ~~entire CanCS region~~ vertically integrated offshore transport of (c) organic and (d) inorganic nitrogen, where positive (red) and negative (blue) shadings represent net offshore and onshore transports, respectively (in ~~our experiment~~Gmol N km^{-1} yr^{-1}).

~~Meridionally integrated net downward and offshore transports of organic (left) and inorganic (right) nitrogen in the upper 200 m as a function of the distance to the coast in the three subregions as well as the entire CanCS in our experiment. Color shading shows the downward transport (in Gmol N km^{-1} yr^{-1}) while contours correspond to the offshore transport (in Gmol N m^{-1} yr^{-1}).~~

Finally, the The offshore transport of organic nitrogen is smaller in magnitude than that of inorganic nitrogen and is mostly limited to the near surface in all subregions (Fig. 10 FIg 7, Fig. S24 and Fig. 9, SIS28). In contrast, the transport of inorganic nitrogen shows a subsurface secondary maximum at between 50 and 100 m in addition to the surface maximum (Fig . 10).

4.5 Horizontal structure of offshore transport

Horizontal distribution of vertically integrated offshore transport of organic (a) and inorganic (b) nitrogen for the whole CanCS region in our experiment. 7, Fig. S24). Our analysis highlights the two opposing effects of subduction in slowing offshore transport speeds but also reducing biological uptake (and nitrogen loss due to sinking) and hence helping maintain high nitrogen content by upwelled water.

The convergence of the Canary coastal current flowing from the north and the Mauritanian current flowing from the south leads to a strong offshore transport of nitrogen around cape Blanc (21°N) (Fig. 11 7 and Fig. 10, SIS29). The nitrogen (both organic and inorganic) channelled through the confluence of the two currents originates predominantly from waters upwelling in the central and southern subregions, with a small contribution from particles upwelling in the northern subregion. This is consistent with the finding of Lovecchio et al. (2017) who - using a Eulerian approach - also found the Cape Verde Front to be a major channel of export of upwelled coastal waters and of the associated nitrogen into the open ocean. Although integrated vertically and averaged in time, the pattern of offshore transport captures a spatially averaged manifestation of mesoscale eddies in latitudinally alternating offshore-onshore corridors known as striations . The emergence of striations has been described in Davis et al. (2014). The pattern also captures the role of filaments in the enhancement of transport at certain capes where there is spatial consistency in coastal filament formation (more in Section 4.1). The presence of striations in offshore flow and the role of filaments in offshore transport have also been documented in Lovecchio (Davis et al.(2017), and the latter has been studied in detail in Lovecchio et al. (2018, 2014).

5 Mechanisms of transport

5.1 Enhancement of offshore transport around capes

The coastal upwelling front associated with the strong density gradient formed at the transition zone between the upwelling waters and the open ocean waters limits the offshore transport. Yet, the cold coastal filaments that emerge from the instability of the upwelling front and its interaction with eddies can play a crucial role in transporting upwelling waters across the front against the mean density gradient. These filaments have been shown to be associated with a high export of organic material and nutrients into the open ocean, particularly in the nearshore. Àlvarez-Salgado et al. (2007) suggested the contribution of filaments to the transport of carbon off Iberia and NW Africa to be 2.5 to 4.5 times larger than the export driven by Ekman transport. Lovecchio et al. (2018) estimate that coastal filaments are responsible for 80% of the offshore transport in the first 100 km offshore. Coastal filaments along the West African coast can occur everywhere, but it is well established that the majority of the filaments are persistently associated with the major capes along the coastcan occur anywhere on the coast in the

CanCS, but previous studies have shown that capes can facilitate their formation (Meunier et al., 2010; Troupin et al., 2012). Lovecchio et al. (2018) demonstrated that in their analyses, 25% of the time, the filaments were associated with capes. Many filaments originating at capes are so persistent and well known that they have been named after the cape, such as the Cape Verde filament (Ndoye et al., 2017; Capet et al., 2017), the Cape Ghir filament (Pelegri et al., 2005b, Troupin et al., 2012) and the exceptionally large and extensive Cape Blanc/Barbas filament that occurs at the confluence of the Canary and Mauritanian currents (van Camp et al., 1991; Barton et al., 2004). Enhanced transport can also be seen at other capes such as Cape Bojador where a persistent filament extending up to 500km offshore can be observed (Figure not shown).

Here, we explore how areas around the major capes that are favorable to strong filamentary activity affect upwelling and offshore export of water and nitrogen. These are Capes Verde (14.5°N - 15.5°N) and Blanc (20°N - 21°N) in the southern subregion, Capes Barbas (22°N - 22.75°N), Bojador (25°N - 26.5°N) and Juby (27.5°N - 28.5°N) in the central subregion and Capes Dra (28.5°N - 29.5°N) and Ghir (30°N - 31°N) in the northern subregion (Fig. ~~4a and Table 2, SI~~1a and Table S2). Previous studies of the Canary upwelling mostly stressed the role of filaments in locally enhancing offshore transport regardless of the source of upwelling. Similarly, we find an enhancement of offshore transport of ~~upwelling~~ upwelled particles in the first 200km from the coast within the latitudinal range of all capes except Capes Verde and Juby (Figure ~~12~~8). Transport at latitudes of capes Blanc, Barbas, Dra and Ghir is larger than at the non-cape latitudes as far as 1000 km from the coast. We further separately consider the enhancement of offshore transport associated with (i) enhanced local upwelling around the capes and (ii) increased export of ~~remotely~~ non-locally upwelled water at each cape, i.e., the export of waters that upwelled far away from the capes but is then transported along the coast toward the cape, from where it is exported toward the open ocean.

The offshore transport of water ~~upwelling~~ upwelled around Cape Bojador in the central subregion and Capes Dra and Ghir in the northern subregion is 20% to 30% larger than that originating from non-cape areas (per coastal length) (Figure ~~11 in SI). Corresponding enhancement in local nitrogen upwelling and export~~ S30). Increased offshore transport of nitrogen due to increased local upwelling is seen only in Capes Dra and Ghir out of the seven capes examined (Figure ~~12~~8). Cape Bojador does not show enhanced local nitrogen upwelling (although a slight enhancement is shown in its offshore export).

Cape Blanc, Cape Barbas and Cape Ghir are highly efficient in exporting ~~remotely~~ non-locally upwelled waters to the open ocean (Fig. ~~12, SI~~S31). Cape Blanc's enhancement of offshore export of nitrogen by ~~remote~~ non-local upwelling compared to the non-cape part of the central subregion is 350% - 400% in the first 400 km then constantly increases further offshore to reach a 935% enhancement at 1200 km. Similarly, Cape Barbas shows an enhancement of ~~remote~~ non-local upwelling of about 200 % for all distances from the coast while Cape Ghir shows a 250% enhancement from 100 km to 800 km offshore (Figure ~~12). The offshore transport of nitrogen by remote upwelling exported by all capes constitutes~~ 8). Non-locally upwelled waters that are transported offshore around major capes represent more than 30% of the total offshore transport ~~of upwelling~~ at all distances from the coast (Fig. ~~7~~ 4 and Fig. ~~12). In fact, all capes source the majority of~~ 8). Indeed, most of the water and nitrogen ~~they export from remote upwelling (Table 3). All capes also source more of their export from remote upwelling compared to the rest of the coast. Remote~~ exported offshore around major capes is non-locally upwelled (Table 2). Each cape also sources more of its export from non-local upwelling than any of the non-cape coastal areas. Non-local upwelling accounts

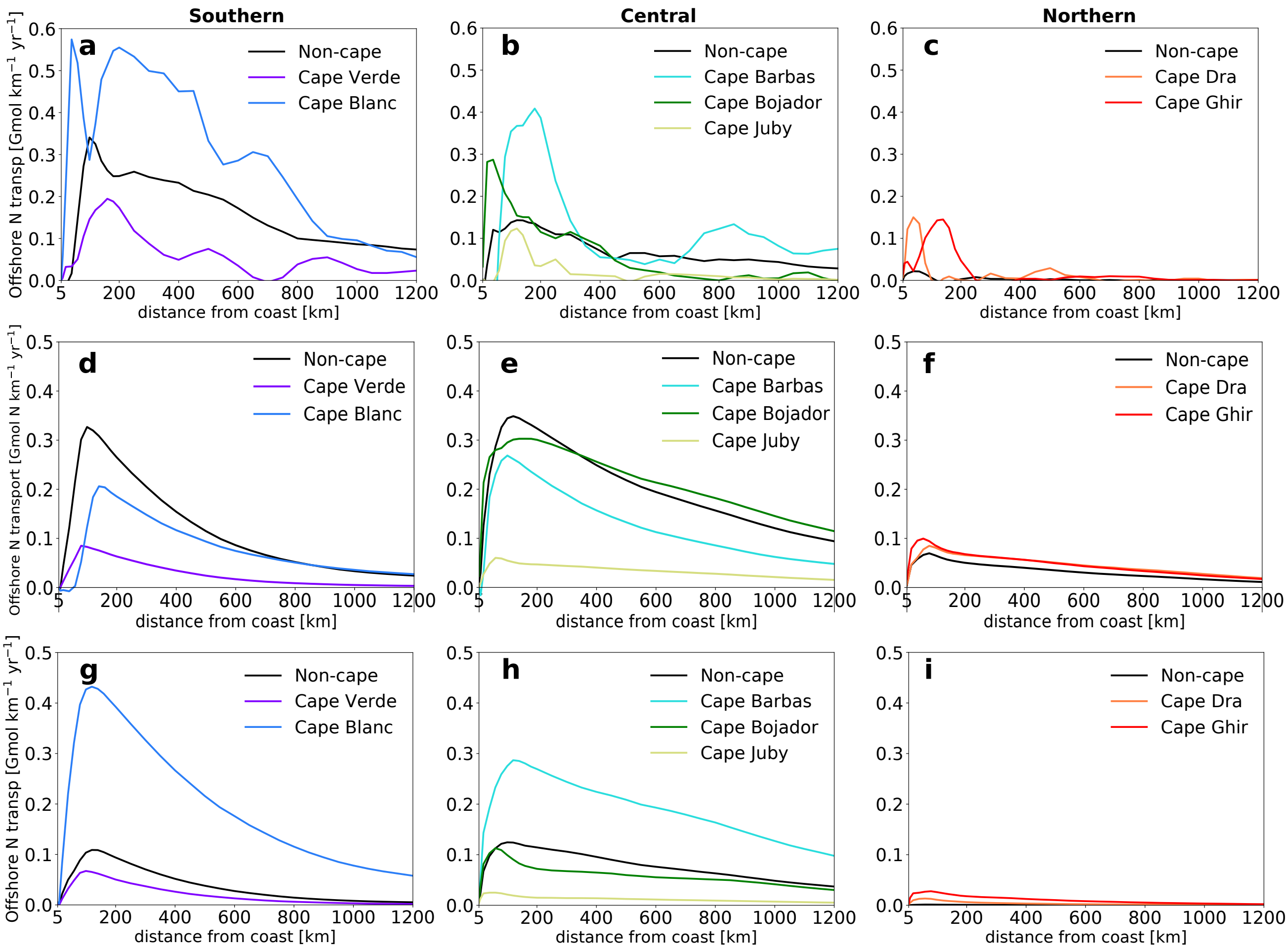

Figure 8. Enhancement of net offshore transport of nitrogen by capes. (a,b,c) Transport within the latitudinal span of each cape or non-cape area. Transport occurring within each latitudinal span is considered at any distance from the coast irrespective of the location of upwelling or coastal export. (d,e,f) Transport ~~by water upwelling~~ associated with locally upwelled water in each cape or non-cape coast. (g,h,i) Transport ~~by particles that leave the coastal upwelling region~~ associated with non-locally upwelled water at each cape or non-cape area~~but upwell remotely~~. Note that the transport is normalized by coastal length (divided by the length of the coast at the respective cape/non-cape).

for over 75% of the nitrogen export in all capes except Cape Verde and Cape Bojador while it accounts for a minority of the source of non-cape parts of the coast except in the central subregion (Table ~~3~~2).

The analysis of the source waters for particles exported around the major capes reveals a strong alongshore transport of upwelled particles that connects upwelling between different coastal regions (Fig. ~~13~~9). This is consistent with previous studies that found strong meridional alongshore advection of nutrients (Carr and Kearns, 2003; Pelegri et al., 2006; Meunier et al., 2010; Troupin et al., 2012; Pastor et al., 2013; Pelegri and Benazzouz, 2015; Auger et al., 2016; Lovecchio et al., 2017). The ability of capes to facilitate offshore export of coastal water through their interaction with alongshore advection has also been previously documented (Meunier et al., 2010; Troupin et al., 2012). With the exception of Cape Blanc and Cape Barbas, most capes export offshore water that mostly first upwells north of their latitude (Fig. ~~13~~9). In the central and northern subregions, this is primarily due to the southward offshore flow by the Canary current. In the southern subregion, ~~the effect of the Mauritanian current~~ both the Canary and Mauritanian currents are important sources for coastal upwelling, particularly during winter (Klenz et al., 2018). This is visible in the northern source of upwelling that leaves the coast at all capes in this subregion and the southern source of upwelling that leaves the coast at Cape Blanc and Cape Barbas ~~that act to concentrate remote upwelling from both the north and the south and channel it offshore (Figure 13~~(Figure 9). We conclude that capes such as Cape Blanc and Cape Barbas act to concentrate and export ~~remotely~~ non-locally upwelled waters, and that this effect is much more important than the occurrence of enhanced local upwelling at the capes.

Cape/Non-cape	Local N (Mmol N km^{-1})	~~Remote~~ non-local N (Mmol N km^{-1})	Local N (%)	Local Water (%)
Verde	12.5	32.8	27.6	21.7
Blanc	35.1	233.0	13.1	11.5
Non-cape (southern)	393.7	220.7	64.1	59.3
Barbas	8.9	83.3	9.6	8.0
Bojador	17.7	41.7	29.8	26.5
Juby	2.4	14.6	13.9	10.5
Non-cape (central)	115.1	200.7	36.5	33.5
Dra	1.1	5.4	17.1	14.1
Ghir	3.1	11.9	20.7	20.3
Non-cape (northern)	12.5	2.6	82.7	87.3

Table 2. First two columns show daily contribution of local and ~~remote~~ non-local upwelling to nitrogen that leaves the coastal region at each cape (in Mmol N km^{-1}) per km of coastal length. The last two columns show the contribution of local upwelling (in %) to total nitrogen and water exported at each cape or non-cape coast.

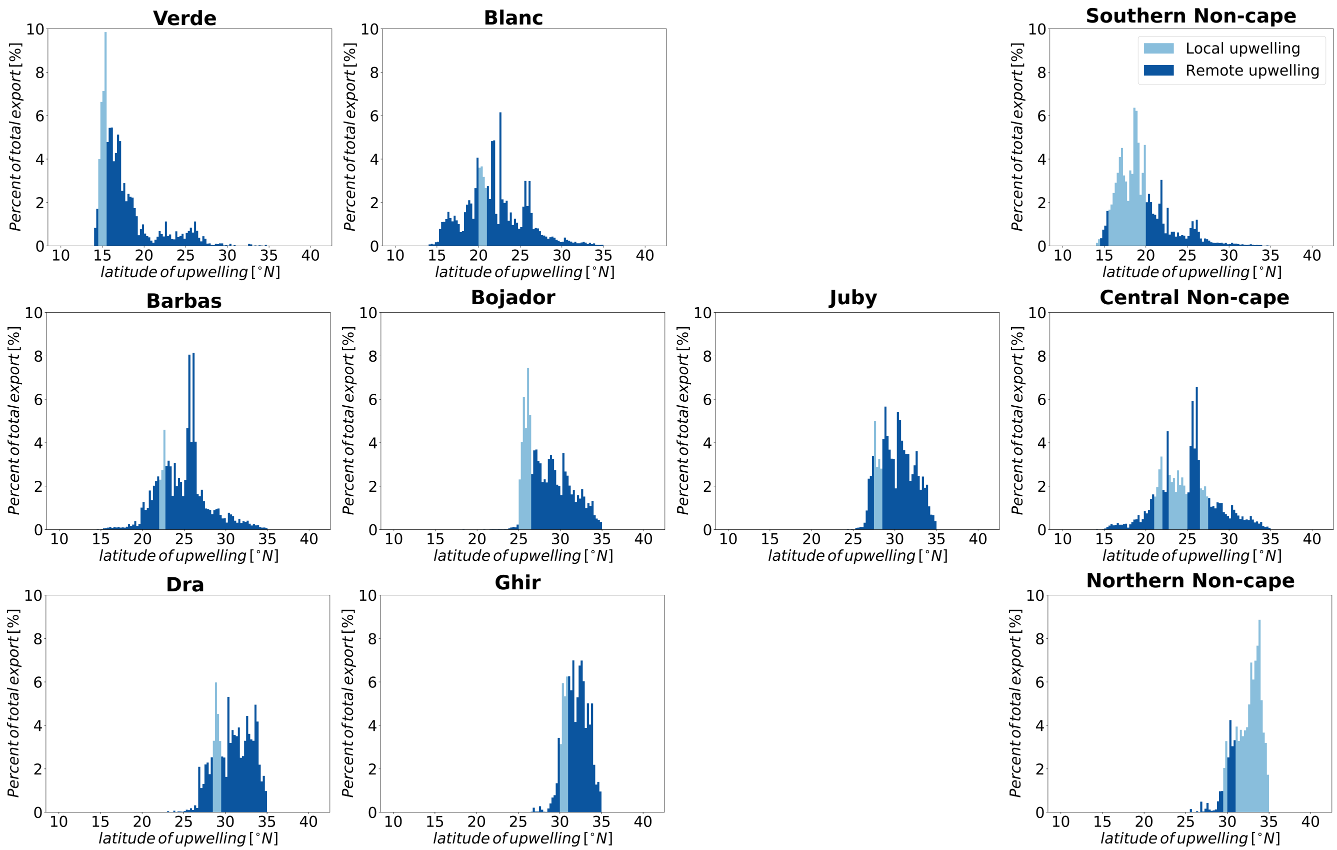

Figure 9. Latitude of upwelling of nitrogen exported at each cape or non-cape coast.

5.2 Role of recirculation

Particles that are transported offshore past a certain distance can return back to that same distance or never cross it again. We term the transport associated with the latter "direct transport". Particles that cross the same distance multiple times can end up further offshore (an odd number of crossings) or closer to the coast (an even number of crossings). We term them "indirect transport" and "net recirculation", respectively (Figure ~~14a~~10a).

It is worth noting that only direct and indirect transport contribute to the net offshore transport of water, while net recirculation does not (although it may slightly contribute to transport of nitrogen) (Figure ~~14~~10). The sum of direct and indirect transports adds up to give the net transport of water to each distance while the sum of all three represents the total volume of water that has reached each distance at any point during the experiment. In the nearshore region, the meandering of the Canary Current as well as the coastal upwelling cell can cause upwelling particles to recirculate closer to the coast (Mittelstaedt and Hamann, 1981; Mittelstaedt, 1983; Estrade et al., 2008). But the leading cause of recirculation in the open ocean is the ~~ubiquitious~~ ubiquitous presence of mesoscale structures, particularly eddies (Mason et al., 2011; Mason et al., 2012; Barton

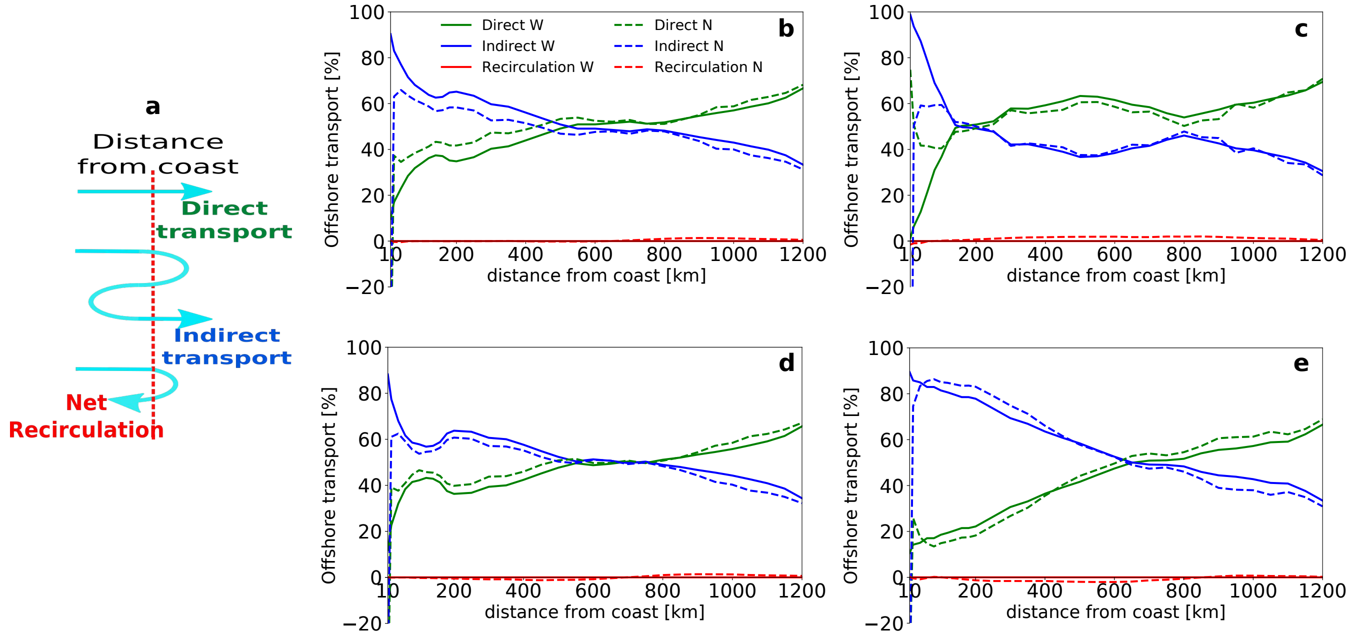

Figure 10. (a) Schematic showing the three types of offshore transport trajectories. (b,c,d,e) Contribution (in %) of direct transport (green), indirect transport (blue) and net recirculation (red) to the total net offshore transport of water (solid) and nitrogen (dashed) at each distance to the coast in the entire CanCS region (b) as well as the southern (c), central (d) and northern (e) subregions. Note that the net recirculation has no contribution to net offshore water transport but contributes slightly to the net offshore transport of nitrogen.

and Aristegui, 2004; Schutte et al., 2016; Kounta et al., 2018; Ndoye et al., 2017; Capet et al., 2017). Therefore, contrasting the direct and indirect components of the transport can be used to gauge the relative importance of the mesoscale eddies and current meandering in the offshore transport.

Examining the three components of the offshore transport in the three subregions reveals that the direct and indirect components virtually explain all the transport of water and nitrogen at all latitudes and distances from the coast. Yet, important differences exist between the three subregions in terms of the relative importance of these two forms of transport (Fig. ~~14). In~~ 10). For the southern subregion ~~, the~~ particles, direct transport contributes by a large share to the total transport of water and nitrogen at all distances except in the first 200 km offshore where the indirect transport dominates. In contrast, for particles upwelled in the central and northern subregions, the direct transport has a greater share to transport only past 700 km offshore, while the indirect transport dominates closer to the coast. The relative importance of ~~the~~ indirect transport is particularly strong between 100 km and 400 km in these two subregions. For instance, at 200 km the indirect transport contributes by up to 65% and 80% to the total offshore transport of water in the central and northern subregions, respectively. For the transport of nitrogen, the share of the indirect transport at the same distance is 60% and 85% in the two subregions.

The importance of the indirect transport of upwelled waters in the central and northern subregions can be linked to the prominent role played by mesoscale eddies there. Indeed, eddies with length scale of 100 km to 300 km are known to be important at these latitudes (Mittelstaedt, 1991). These include a recurrent cyclonic eddy south of Cape Juby and the cyclonic and anticyclonic eddies entrained by the Canary Archipelago, forming the so called Canary Eddy Corridor (CEC), which is located at $22° - 29°$ (Arístegui et al., 1994; Piedeleu et al., 2009; Sangrà et al. 2009). This region of long-lived westward-propagating eddies is known to contribute strongly to the offshore transport of organic matter and carbon (Sangrà et al., 2009). Yet, the transport pathway of upwelling from the southern subregion has also been previously shown to feature significant eddy activity (Schutte et al., 2016; Kounta et al., 2018; Ndoye et al., 2017; Capet et al., 2017).

The prominence of water recirculation in the central and northern subregions - materialized by the dominance of the indirect transport - up to 600-800 km offshore is consistent with the longer crossshore transit times characterizing these latitudes (~~Table 2~~ Fig 3 and Fig. ~~13, SI~~S32). This suggests that recirculation acts to slow down the offshore transport and may explain the less efficient offshore transport of water upwelling from these regions (Fig. ~~7a~~4a).

6 Potential contribution to open ocean nitrogen budget

The strong export of nutrients and organic matter from the ~~CanUS~~ CanCS to the oligotrophic open ocean fuels new production (NP) and contributes to heterotrophy there. Here we quantify this contribution in the North Atlantic Tropical Gyral Province (NATR) and the North Atlantic Subtropical Gyral East (NASE) provinces as defined by Longhurst et al. (2007) (see Fig. ~~3 in SI~~S20). The Lagrangian approach allows for the isolating of the contribution of the upwelling particles to the transport of nitrogen into the NATR and NASE provinces, adjacent to the ~~CUS~~ CanCS (see Fig. ~~3, SI).~~ S20). We calculate the net offshore transport of nitrogen in the top 100 m at the precise boundaries between each CanCS subregion and each Longhurst province.

~~NP~~ New Production (NP) is estimated from the Net Primary Production (NPP) and the available estimates of the f-ratio (f-ratio= $\frac{NP}{NPP}$) in the literature. ~~NPP is derived in each province from~~ Since new production and export production (EP) are numerically the same in a system in steady-state (Dunne et al. 2006), we also use estimates of the e-ratio (e-ratio= $\frac{EP}{NPP}$). For NPP, we use the Vertically Generalized Production Model (VGPM) ~~using~~ estimates, based on sea color data from 1997 to 2017~~(Table 4~~, as well as a carbon-based productivity model (CbPM) by Westberry et al. (2008) to derive NPP for each province. We also use an in-situ estimate of NPP for the NATR made by Tilstone et al. (2009) based on Carbon-14 uptake (Table 3). We use estimates of the f-ratio from Laws et al. (2000) (see their Plate 3) as well as previous estimates of the ~~export efficiency (i.e., e-factor)~~ eratio from Henson et al. (2011) and Siegel et al. (2014)~~since the two are equivalent for sufficiently large open ocean regions (Eppley and Peterson, 1979)~~. The derived f-ratio values are typically low and vary from 4% in the NATR according to Henson et al. (2011) to 15% in the NASE following Laws et al. (2000) (Table ~~4~~3).

The southern, central and northern coastal upwelling subregions in our study have total upwellings of 282.3, 200.9 and 79.2 Gigamol N yr^{-1}, respectively. ~~From this total of 562.4~~ A total of 563 Gmol N yr^{-1}, ~~357.6~~ 358 Gmol N yr^{-1} and ~~32.4~~ 32 Gmol N yr^{-1} reach the upper 100m of the NATR and the NASE, respectively. When normalized by the area of each province, the CanCS upwelling source corresponds to ~~43.7~~ 44 mmol N m^{-2} yr^{-1} and ~~7.3~~ 7 mmol N m^{-2} yr^{-1} for the NATR and NASE,

Table 3. Nitrogen supply to sources and sinks for the NATR and NASE provinces (in mmol N m^{-2} yr^{-1}). Sources considered are the offshore transport by the Canary upwellingand other sources and , the estimated net meridional transfer of nitrogen through Ekman divergence, N_2-fixation and atmospheric deposition. The only sink considered is new production (NP)in the two provinces. Contribution of upwelling by each subregion is calculated by adding the net amount of nitrogen upwelling particles carry to each province in the top 100 m by the end of the experiment.

N source	NATR	NASE
Canary upwelling		
Deep source		
14-21°N	14.5	> 0.0
21-28°N	18.2	1.5
28-35°N	3.8	4.8
Total	36.5	6.3
Shallow source		
14-21°N	4.3	> 0.0
21-28°N	2.1	0.1
28-35°N	0.8	0.8
Total	7.2	1.0
NPP (VGPM) 1753 2139 NP New Production		
Laws et al. (2000)* (e-factoref-ratio=0.06, 0.16)	105.2 83-120	342.2 320-342
Siegel et al. (2014)* (e-factoref-ratio=0.08 for both)	140.2 110-160	171.1 160-171
Henson et al. (2011)* (e-factoref-ratio=0.04, 0.07)	70.1 55-80	149.7 140-150
N_2 biological fixation		
Luo et al. (2012)	22.5 ± 12.5	1.5 ± 0.4
Moore et al. (2009)*	23	< 3
Fernández-Castro et al. (2015)	3.1 ± 2.4	2.5 ± 1.1
Atmospheric deposition (Duce et al., 2008)	9.5 ± 2.5	14.5 ± 2.5
Net meridional transfer (Williams and Follows, 1998)	30 (NO_3 only)	30 (NO_3 only)

* estimates are based on maps provided by the cited paper

** Contribution of upwelling by each subregion is calculated by adding the net amount of nitrogen upwelling particles carry to each province in the top 100 m by the end of the experiment. That is, whenever a particle enters a province within the top 100m, the nitrogen it carries into the province is added to the particle's source subregion's contribution to the province. On the contrary, when a particle from a given subregion leaves a province within the top 100m, the nitrogen it carries with it when it leaves the province is subtracted from the contribution of the subregion of the particle to the province.

respectively (Table 43). Most of the upwelled nitrogen exported to The NATR originates from the central (46.5%) and southern subregions (43%), whereas the nitrogen upwelled in the northern subregion dominates (76.7%) the nitrogen supplied to the NASE. Hence, the nitrogen transported (in the top 100m) from the Canary coastal upwelling to the NATR and NASE provinces represents 31.2 27 - 62.3 % and 2.1 79 % and 2 - 4.95 % of their total NP, respectively , based on NP values calculated from Laws et al. (2000), Siegel et al. (2014) and Henson et al. (2011New production, respectively (Table 3).

Finally, the contribution of the Canary upwelling also appears significant in comparison to other major sources of new nitrogen to the oligotrophic open North Atlantic Ocean such as N_2 fixation (Moore et al, 2009; Luo et al., 2012; Fernandez-Castro et al., 2015), atmospheric deposition (Duce et al., 2008) and net meridional transfer through Ekman divergence (Williams and Follows, 1998). Indeed, the upwelling source seems to exceed contributions from N_2 fixation, the atmospheric deposition and meridional transfer in the NATR province. In the NASE province, the upwelling contribution is larger than the N_2 fixation but weaker than the atmospheric deposition and the meridional transfer (Table 43).

7 Comparison with previous studies

Comparison of POC offshore transport estimates in the CanCS region from previous studies and from the present study. Note that our model-based estimates correspond to annual mean climatologies whereas observation-based estimates listed in the table are based on data collected from different individual campaigns that took place either in August or September. All values are given in kg C s^{-1} with a C:N ratio of 6.625 assumed in our model.

Previous study Latitude Longitude (offshore dist.) Depth Time Transportestimate Thisstudy Alonso-González et al. (2009) 20°N-29.2°N 20.35°W 0m-73m 7-29 Sep, 2003 161.3 109.8 - 26°W 0m-135m - 212.7 40.3 García-Muñoz et al. (2004) 27.6°N-27.85°N 13.7°W 0m-100m 13-26 Aug, 1999 18.8 10.6 García-Muñoz et al. (2005) 30.8°N-32.4°N 11.25°W 0m-100m 26 Sep-2 Oct, 1997 11.2 5.6 Santana-Falcon et al. (2016) 30.2°N-31.2°N 10.6°W 0m-100m 26-27 Aug, Many previous studies reported higher estimates of POC offshore export in several portions of the CanCS (e.g.: Alonso-González et al., 200920.9 3.4 Lovecchio et al. (2017) 17°N-24.5°N 100km 0m-100m Annual mean 404 273.3 - 500 km - 207 176.8 - 1000 km - 70 61.1 24.5°N-32°N 100km - 198 93.2 - 500 km - 34 16.1 - 1000 km - 11 3.2

Several previous studies of the CanCS estimated the offshore transport of particulate organic carbon (POC) at various locations off the Northwest African coast (Table 5). For instance, Alonso-González et al. (2009) derived estimates of offshore transport of suspended POC in the upper ocean in a box model approach using in-situ measurements of POC and velocities based on geostrophy and Ekman contribution computed from remotely sensed estimates. The POC export was quantified between 20°N and 29.2°N at two different transects at 20.6° W and 26° W for the top water column with a density of 26.44 kg m^{-3} or less. Their transport estimates exceed ours by around 45% and a factor five at 20.6° W and 26° W, respectively (Table 5).These discrepancies might result from the important sampling differences between the two studies, as our estimates correspond to annual-mean climatologies and are restricted to waters that upwell near the coast in contrast to the observational study.We also note that the mismatch between the two studies is particularly large for the deeper (0-135 m) and the further offshore (26° W) transect that is more likely to be affected by waters not directly related to coastal upwelling.García-Muñoz et al. (2004) and ; García-Muñoz et al.(, 2004; García-Muñoz et al., 2005) estimated the offshore transport of POC in the top 100 m associated with two filaments near C. Juby and C. Ghir, respectively. These estimates are nearly twice as large as ours (Table 5).Similarly, ; Santana-Falcon et al.(, 2016) inferred the offshore transport of POC associated with a filament near C. Ghir observed in August 2009 (Table 5). Their estimate exceeds our model-based annual-mean offshore transport estimate by almost a factor six (Table 5). Finally, we contrast annual mean POC offshore transport estimates by ; Lovecchio et al.(2017) to ours. While the transport figures by the two studies are relatively close between 17°N and 24.5°N at large offshore distances (> 500 km), our estimated transport is nearly twice weaker in the nearshore and up to three times smaller at 1000 km between 24.5°N and 32°N (Table 5). While Lovecchio et al. (, 2017) is the only previous study that provides model-based large-scale annual mean estimates of the offshore transport of POC in the CanCS, it is based on Eulerian approach that does not distinguish between waters that originate from the coastal upwelling and the non-upwelling waters.

In summary, all previous studies reported here find higher estimates of POC offshore export in several portions of the CanCS. ; more in Table S4). Our lower offshore transport estimates may at least partially result from our Lagrangian approach that focuses on coastally upwelled water only, disregarding non-upwelling waters and open ocean upwelling. Furthermore, restricting the analysis to upwelling particles in our study limits offshore flux to near-surface waters as most upwelled waters remain at very shallow depth . Finally, the loss of organic nitrogen due to sinking of particulate matter experienced by upwelling waters as they are exported offshore likely contributes to our overall lower transport estimates(see section in supplementary material for more detail).

Previous model-based studies of the Benguela and California coastal upwelling systems suggest other EBUS may also significantly contribute to the nitrogen budget of adjacent open oceans (Table 4, SIS5). For instance, Gutknecht et al. (2013) found significant net offshore transport of nitrogen in the Benguela current system (BenCS), with organic nitrogen exceeding inorganic nitrogen at far offshore distances. They estimated the contribution of the BenCS in the top 50m, to amount to 100 $\pm$ 40 mmol N m^{-2} yr^{-1} to the adjacent South Atlantic Subtropical Gyral Province according to the classification by Longhurst (2007) (Gutknecht et al., 2013). This contribution, however, is likely overestimated since results in the highly productive Walvis Bay area (22°S-24°S) were linearly extrapolated to the whole BenCS. Frischknecht et al. (2018) also found high offshore export of both organic and inorganic nitrogen from the productive central region of the California current system (CalCS) to the open ocean as far as 500 km from the coast (Table 4, SIS5). The efficiency of offshore transport of organic matter and dissolved inorganic nitrogen in the top 100 m between 100 km and 500 km are almost identical between their study of the CalCS and the present study of the CanCS.

8 Implications and caveats

Our Lagrangian approach identified waters upwelling along the Northwest African coast and characterized the kinetics, structure and timescale of their offshore transport. Using a Lagrangian approach allowed us to assess the reach and fate of coastally upwelled nitrogen far from the coast as well as study its biogeochemical transformation along particle trajectories. Our estimate of offshore export of organic nitrogen/carbon by upwelling is lower than the estimate by Lovecchio et al. (2017), at all distances from the coast (Table ~~3 in SI~~S3). These differences can in particular stem from the differences in approaches (Lagrangian vs. Eulerian) and the studied parts of the CanCS (their budget is computed for the area between 9.5°N and 32°N) that differ between the two studies. We found the offshore transport to be generally slowest in the first few hundreds of km from the coast and to increase in speed with increasing offshore distances (~~Table 2~~Fig 3). This is particularly true for waters upwelling in the northern and the southern subregions of the CanCS. The existence of an inverse relationship between upwelling water recirculation and their cross-shore transit times (Fig. ~~13, SI~~S32) suggests the slowdown of offshore transport in the first 300-500km to result from a larger role played by eddies that act to weaken the net offshore transport there. Previous studies have highlighted the role of eddies in contributing to organic carbon and nutrient offshore transport in EBUS (Nagai et al., 2015; Lovecchio et al., 2018). The findings of the present study reveal that enhanced water recirculation driven by intense eddy activity may reduce the efficiency of the offshore transport of water.

In the first 200km, the offshore transport is fastest and the water recirculation is weakest for particles that upwelled in the central CanCS subregion (~~Table 2~~Fig 3, Fig. ~~13, SI~~S32). We show that this region is characterized by the presence of major filament-generating capes such as Cape Blanc and Cape Barbas that contribute strongly to offshore transport of water and nutrients. They act as concentrators that collect coastal water and ~~nutrient~~ nutrients and channel it to the open ocean as most of the water exported (84%) at the capes upwells ~~remotely~~non-locally. Lovecchio et al. (2018) have highlighted the role of persistent filaments in mediating more than 80% of the offshore transport of organic carbon in the first 100km from the coast. Here, we show that key capes along the CanCS represent hotspots of offshore transport of water and nitrogen, thanks to the intense filaments that develop around them. Our findings also highlight the importance of the alongshore transport as most of the waters exported at capes have upwelled at latitudes far away from the location of the capes. This is consistent with the concept of the three-dimensional biological pump highlighted in previous studies, according to which strong offshore and alongshore lateral transports decouple the locations of upwelling and of biological export (Plattner et al., 2005; Lovecchio et al. 2017, 2018).

As the along-trajectories nitrogen-depletion rates depend on the depth of the transport, the subduction of upwelling waters to deeper layers occurring mostly between 100 and 200km offshore tends to affect the efficiency of the offshore transport of nitrogen. For instance, in the southern subregion where the transport is the shallowest, the nitrogen depletion is large (because of biological uptake and sinking), thus resulting in smaller supply of upwelled nitrogen to the North Atlantic gyre at large distances from the coast. Conversely, the northern and central subregions contribute relatively more to the open ocean nitrogen supply due to deeper transport and weaker nitrogen-depletion.

Finally, our study confirms the strong alongshore variations of the CanCS in terms of offshore transport reach and efficiency. Our results show that the offshore transport of nitrogen off the CanCS depends on many important factors, including the intensity of upwelling, the efficiency of the offshore transport, controlled by the kinetics of the transport and the nitrogen depletion rates. In particular, factors such as eddies, filaments, and alongshore transport all contribute to modulate the magnitude and reach of the water volume and nutrient content transported offshore. The complexity of these factors and their interactions explain the complexity of the offshore transport and its spatial diversity.

Yet, the study has several caveats that stem from the limitations of the experimental design or are inherent to the tools. ~~For instance~~The physical model underestimates EKE in parts of the domain, including in the southernmost part. This may be in part due to the monthly climatology wind forcing we use, potentially leading to an underestimation of vertical mixing and an incomplete representation of the complex upwelling dynamics. However, our analysis shows that the model successfully captures much of the spatial and seasonal variations in upper ocean mixing (Fig S1) and reproduces upwelling distributions and pathways that are not inconsistent with previous findings. On the other hand, our biogeochemical model is based on nitrogen and has no representation of other potentially limiting nutrients such as iron and phosphate. Furthermore, the model lacks a representation of nitrogen fixation. Yet, previous studies indicate nitrogen to be the main limiting nutrient (e.g., Moore et al., 2013) and nitrogen fixation to be very low (Luo et al., 2012; Moreira-Coello et al., 2017) in the CanCS upwelling region. Also, the model only has one class of phytoplankton. However, the specific nature of the phytoplankton community appears to be of secondary importance as our model reproduces quite well the mean vertical profiles of POC in different parts of the domain (Fig S15). Therefore, we believe these ~~model limitations~~ limitations in the biogeochemical component of the model should not affect the study's main conclusions.

A potentially more serious limitation stems from our Ariane-based Lagrangian analysis~~that~~. First, ARIANE includes resolved transport but does not explicitly take into account subgrid mixing in the computation of trajectories. This is a common problem in most Lagrangian trajectory based studies. We think including subgrid mixing should increase the vertical dispersion of upwelled water and nitrogen. While this may reduce the offshore transport efficiency (weaker offshore velocities at depth), it should also reduce along-trajectory nitrogen depletion. A compensation (even partial) between these two processes may lead to an overall small change in the estimated total supply of upwelled nitrogen to the open North Atlantic ocean. Yet in contrast to water volume, tracing the transport of nitrogen is somewhat more difficult given the chemical transformations between inorganic and organic nitrogen. Yet, as has been shown also by Frischknecht et al. (2018), the Lagrangian method permits a lot of new insight into the offshore transport of nitrogen, since total nitrogen, i.e., the sum of inorganic and organic nitrogen is conserved except for the part that is sinking. The component we lose through sinking does not affect our conclusions, since this component is lost to the ocean interior, from where it will not find its way back into the waters that are transported offshore. More importantly is our lack of consideration of the vertical mixing. We have good evidence that this component is relatively small. If the supply of nitrogen from surrounding waters to upwelling waters due to mixing were large enough to cancel the loss due to organic matter sinking, there would be no such a sharp decline in total nitrogen as a function of distance to the coast relative to that for water volume (Fig 4). Moreover, this decline is larger for water particles originating from the southern subregion that are transported at the shallowest depths and that are subject to the strongest sinking loss (Fig S23). This suggests that although the potential changes in nitrogen due to subgrid mixing can locally be important, they are unlikely to affect the large-scale transport estimates in a significant way.

~~Finally~~Furthermore, our coastal upwelling sampling involves subjective choices that can in theory affect our results. For instance, the identification of upwelling waters based on the upward crossing of a constant depth (70 m) is a somewhat arbitrary choice. Some previous Lagrangian studies have used cold sea surface temperature to identify and track upwelling waters (e.g. Rivas and Samelson, 2011). However, such definitions can be misleading as cold waters not necessarily associated with upwelling may also be sampled. In the present study, our approach is based on the use of vertical velocities to identify upwelling. More specifically, we use the crossing of the 70 m depth as this corresponds to the average depth of the euphotic zone in the Canary coastal region. However, both upwelling depth and the depth of the euphotic zone vary in space and time. Yet, Drake et al. (2018) show that defining upwelling with varying depth criteria yield yields results that are also well captured by experiments that use fixed depths. Furthermore, a variable upwelling depth definition can make it difficult to distinguish between upwelling variations driven by the variability of atmospheric forcing and those caused by changes in the analysis depth.

It is worth noting that only coastal waters that originate from the open ocean are sampled as particles are released at the western section of the coastal region only. Therefore, water that may enter the control box However, we have found that only a very small amount of water, 1% and 3% of the total volume tracked in this study, enters the upwelling coastal region along the coast from the north or the south is not considered. Excluding waters that enter along the shelf restricts our analysis to upwelling waters that carry deep ocean properties. Because of northern and southern boundaries, respectively. Furthermore, given the high rate of recirculation near the coast, a vast proportion of the particles that may have entered the coast alongshore, once upwelled and exported offshore, are likely to return to the much extended western section in comparison to the northern and southern exits, we believe this potentially missing influx of coastal water to be small and unlikely to affect our results.

9 Summary and conclusions

We quantify the offshore export of water and nitrogen from the CanCS using a Lagrangian approach that consist in tracking all open oceancoast from the open ocean, in which case they would be sampled in our particle release. Therefore, discarding particles entering the coastal region and upwelling along the West African coast between 14°N and 35°N. ocean from the southern and northern boundaries of the upwelling strip is likely to cause only a limited error in our quantification of the offshore transport.

9 Summary and conclusions

Due to a larger upwelling volume and a faster offshore transport in the nearshore region (up to 400 km offshore), the central CanCS subregion is responsible for the largest net offshore transport of water at any distance from the coast. Conversely, the southern CanCS is associated with the smallest offshore transport up to 800 km offshore due to a smaller volume of coastal upwelling. Yet, the southern subregion exports the highest amount of nitrogen offshore at 200 km because of a large upwelling flux of nitrogen associated with a shallower thermocline and higher subsurface nitrogen concentration. At larger distances from the coast, the offshore transport of nitrogen associated with the central subregion exceeds that originating from the southern subregion because of a lower nutrient depletion caused by a more frequent subduction of upwelled water into deeper layers where phytoplankton growth is light-limited. The analysis of nitrogen allocation along trajectories reveals that the offshore transport of organic nitrogen is generally less than half of that of inorganic nitrogen and is mostly limited to the near surface in all subregions.

The pattern of offshore transport is characterized by the presence of latitudinally alternating offshore-onshore corridors indicating a strong contribution of mesoscale eddies and filaments to the mean transport. Major capes along the CanCS that are favorable to the formation of persistent filaments are associated with an enhanced offshore export of water and nitrogen. This results primarily from an enhancement of local export of water and nitrogen ~~remotely~~ non-locally upwelled (by up to a factor 4 to 9 for C. Blanc) relative to non-cape areas. The offshore transport of nitrogen by ~~remote~~ non-local upwelling exported by all capes constitutes more than $\frac{1}{3}$ of the total offshore transport of upwelling waters at all distances from the coast. All capes source the majority of water and nitrogen they export from ~~remote upwelling. In the southern CanCS, most upwelled water and nitrogen traveling beyond 200 km from the coast are transported further offshore with no recirculation back to the coast. In contrast, the majority of water particles that upwell in the central (up to 65%) and northern (up to 80%) CanCS transported offshore recirculate back to closer offshore distances in the area between 100 and 500 km offshore. This reflects the larger role played by recurrent mesoscale eddies in these regions. This enhanced recirculation results in an increase of the cross-shore transit times and a reduction in the efficiency of the offshore transport.~~ non-local upwelling.

Finally, we found the supply of nitrogen by the Canary upwelling to the NATR and the NASE provinces, to amount to 43.7 mmol N $m^{-2}yr^{-1}$ and 7.3 mmol N $m^{-2}yr^{-1}$, respectively. This represents ~~45~~53±~~15~~26% and 3.5±1.5% of the total potential new production in the two provinces, respectively The contribution of the Canary upwelling appears significant in comparison to other major sources of new nitrogen to the open North Atlantic Ocean. This emphasizes the importance of the CanCS upwelling in particular and EBUS in general as a key source of ~~nutrient~~ nutrients to the open ocean and the offshore transport as a mechanism of supply of these nutrients to the adjacent oligotrophic gyres~~, stressing~~ . Our work thus stresses the need for improving their representation in global coarse resolution models, as has been indicated by previous works (e.g., Large and Danabasoglu, 2006).

Acknowledgements. Support for this research has come from the Center for Prototype Climate Modeling (CPCM), the New York University Abu Dhabi (NYUAD) Research Institute. Computations were performed at the High Performance cluster (HPC) of NYUAD, Dalma. NG acknowledges support by the Swiss National Science Foundation through the CALNEX project (Grant 149384) and by the Swiss Federal Institute of Technology Zurich (ETH Zurich). The authors are also grateful to Michael Mehari for producing the Taylor diagrams presented in this work. We thank two reviewers for their constructive comments that helped to improve and focus our paper. The authors are grateful to B. Blanke and N. Grima for making their ARIANE code available and to the NYUAD HPC team for technical support. The authors declare that they have no competing financial interests. The model code can be accessed online (http://www.romsagrif.org).

References

Alonso-González, I. J., Arístegui, J., Vilas, J. C., and Hernández-Guerra, A.: Lateral POC transport and consumption in surface and deep waters of the Canary Current region: A box model study, Global Biogeochemical Cycles, 23(2), 2009.

Àlvarez-Salgado, X. A., Arístegui, J., Barton, E. D., and Hansell, D. A.: Contribution of upwelling filaments to offshore carbon export in the subtropical Northeast Atlantic Ocean, Limnology and Oceanography, 52, 1287–1292, doi:10.4319/lo.2007.52.3.1287, 2007.

Arístegui J., Sangrà P., Hernández-León S., Cantón M., Hernández-Guerra A., Kerling J. L.: Island-induced eddies in the Canary Islands, Deep-Sea Res., 49, 1087-1101, 1994.

Arístegui, J., Tett, P., Hernández-Guerra, A., Basterretxea, G., Montero, M. F., Wild, K., Sangrá, P., Hernández-León, S., Canton, M., García-Braun, J. A. and Pacheco, M.: The influence of island-generated eddies on chlorophyll distribution: a study of mesoscale variation around Gran Canaria, Deep Sea Research Part I: Oceanographic Research Papers, 44(1), 71-96, 1997.

Arístegui J., Barton E. D., Álvarez-Salgado X. A., Santos A. M. P., Figueiras F. G., Kifani S., Hernández-León S., Mason E., Machú E., and Demarcq H.: Sub-regional ecosystem variability in the Canary Current upwelling, Prog. Oceanogr., 83, 33-48, 2009.

Auger, P. A., Gorgues, T., Machu, E., Aumont, O., and Brehmer, P.: What drives the spatial variability of primary productivity and matter fluxes in the north-west African upwelling system? A modelling approach, Biogeosciences, 13(23), 6419-6440, 2016.

Aumont, O., Maier-Reimer, E., Blain, S., and Monfray, P.: An ecosystem model of the global ocean including Fe, Si, P colimitations, Global Biogeochem. Cy., 17, 1060, https://doi.org/10.1029/2001GB001745, 2003.

Baker, A. R., Lesworth, T., Adams, C., Jickells, T. D., and Ganzeveld, L.: Estimation of atmospheric nutrient inputs to the Atlantic Ocean from 50 N to 50 S based on large-scale field sampling: Fixed nitrogen and dry deposition of phosphorus, Global Biogeochemical Cycles, 24(3), 2010.

Barnier, B., Siefridt, L., and Marchesiello, P.: Thermal forcing for a global ocean circulation model using a three-year climatology of ECMWF analyses, Journal of Marine Systems, 6(4), 363-380, 1995.

Barton, E.: Meanders, eddies and intrusions in the thermohaline, Oceanol. Acta, 10(3), 267-283, 1987.

Barton, E. D.: The poleward undercurrent on the eastern boundary of the subtropical North Atlantic, in: Poleward Flows Along Eastern Ocean Boundaries, Coastal and Estuarine Studies, Springer, 34., 82-95, 1989.

Barton, E., Arístegui, J., Tett, P., Canton, M., Garcia-Braun, J., Hernández-León, S., Nykjaer, L., Almeida, C., Almunia, J., Ballesteros, S., Basterretxea, G., Escanez, J., Garcia-Weill, L., Hernández-Guerra, A., LópezLaatzen, F., Molina, R., Montero, M., Navarro-Perez, E., Rodriguez, J., van Lenning, K., Vélez, H., and Wild, K.: The transition zone of the Canary Current upwelling region, Progress in Oceanography, 41, 455–504, doi:10.1016/S0079-6611(98)00023-8, 1998.

Barton, E. D. and Arístegui, J.: The Canary Islands coastal transition zone–upwelling, eddies and filaments, Progress in Oceanography, 62, 67-69, 2004.

Barton, E. D., Arístegui, J., Tett, P., and Navarro-Pérez, E.: Variability in the Canary Islands area of filament-eddy exchanges, Progress in Oceanography, 62(2-4), 71-94, 2004.

Basterretxea, G. and Aristegui, J.: Mesoscale variability in phytoplankton biomass distribution and photosynthetic parameters in the Canary-NW African coastal transition zone, Marine Ecology Progress Series, 197, 27-40, 2000.

Bettencourt, J. H., Rossi, V., Hernández-García, E., Marta-Almeida, M., and López, C.: Characterization of the structure and cross-shore transport properties of a coastal upwelling filament using three-dimensional finite-size Lyapunov exponents, Journal of Geophysical Research: Oceans, 122(9), 7433-7448, 2017.

Blanke, B. and Raynaud, S.: Kinematics of the Pacific Equatorial Undercurrent: An Eulerian and Lagrangian Approach from GCM Results, Journal of Physical Oceanography, 27, 1038–1053, doi:10.1175/1520-0485(1997)027<1038:KOTPEU>2.0.CO;2, 1997.

Bonnet, S., Caffin, M., Berthelot, H., and Moutin, T.: Hot spot of N2 fixation in the western tropical South Pacific pleads for a spatial decoupling between N2 fixation and denitrification, Proceedings of the National Academy of Sciences, 114(14), E2800-E2801, 2017.

Brink, K. H. and Cowles, T. J.: The coastal transition zone experiment, Journal of Geophysical Research, 96, 14637-14647, 1991.

Brochier, T., Mason, E., Moyano, M., Berraho, A., Colas, F., Sangrà, P., Hernández-León, S., Ettahiri, O., and Lett, C.: Ichthyoplankton transport from the African coast to the Canary Islands, Journal of Marine Systems, 87(2), 109-122, 2011.

Bryden, H. L., Brady, E. C., and Pillsbury, R. D.: Flow through the Strait of Gibraltar, Seminario sobre la Oceanografia fisica del Estracho de Gibraltar, 166-194, 1988.

Capet, X. J., Marchesiello, P., and McWilliams, J. C.: Upwelling response to coastal wind profiles, Geophys. Res. Lett., 31, L13311, doi:10.1029/2004GL020123, 2004.

Capet, X., Estrade, P., Machu, É., Ndoye, S., Grelet, J., Lazar, A., Marié, L., Dausse, D., and Brehmer, P.: On the dynamics of the southern Senegal upwelling center: observed variability from synoptic to superinertial scales. Journal of Physical Oceanography, 47(1), 155-180, 2017.

Carr, M.-E.: Estimation of potential productivity in Eastern Boundary Currents using remote sensing, Deep Sea Research Part II: Topical Studies in Oceanography, 49, 59–80, doi:10.1016/S0967-0645(01)00094-7, 2001.

Carr M.-E. and Kearns E. J.: Production regimes in four Eastern Boundary Current systems, Deep-Sea Res., 50, 3199-3221, 2003.

Chavez, F. P. and Messié, M.: A comparison of Eastern Boundary Upwelling Ecosystems, Progress in Oceanography, 83, 80–96, doi:10.1016/j.pocean.2009.07.032, 2009.

Cropper, T. E., Hanna, E. and Bigg, G. R.: Spatial and temporal seasonal trends in coastal upwelling off Northwest Africa, 1981–2012, Deep Sea Research Part I: Oceanographic Research Papers, 86, 94-111, 2014.

da Silva, A.M., Young, C.C. and Levitus, S.: Atlas of surface marine data 1994, Vol. 3, Anomalies of heat and momentum fluxes, NOAA Atlas NESDIS, 8, 411, 1994.

da Silva, A.M., Young, C.C. and Levitus, S., 1994. Atlas of surface marine data 1994, Vol. 4: Anomalies of fresh water fluxes, NOAA Atlas, NESDIS, 9, 1994.

Davis, A., Di Lorenzo, E., Luo, H., Belmadani, A., Maximenko, N., Melnichenko, O., and Schneider, N.: Mechanisms for the emergence of ocean striations in the North Pacific, Geophysical Research Letters, 41, 948–953, doi:10.1002/2013GL057956, 2014.

Del Giorgio, P. A., Cole, J. J., and Cimbleris, A.: Respiration rates in bacteria exceed phytoplankton production in unproductive aquatic systems, Nature, 385(6612), 148-151, 1997.

Del Giorgio, P. A. and Duarte, C. M.: Respiration in the open ocean, Nature, 420, 379–384, https://doi.org/10.1038/nature01165, 2002.

Dentener, F., Drevet, J., Lamarque, J. F., Bey, I., Eickhout, B., Fiore, A. M., Hauglustaine, D., Horowitz, L. W., Krol, M., Kulshrestha, U. C., and Lawrence, M.: Nitrogen and sulfur deposition on regional and global scales: a multimodel evaluation, Global biogeochemical cycles, 20(4), 2006.

Diaz, F. and Raimbault, P.: Nitrogen regeneration and dissolved organic nitrogen release during spring in a NW Mediterranean coast zone (Gulf of Lions): Implications for the estimation of new production, Mar. Ecol. Prog. Ser., 197, 51–65, doi:10.3354/meps197051, 2000.

Dore, J. E. and Karl, D. M.: Nitrification in the euphotic zone as a source for nitrite, nitrate and nitrous oxide at Station ALOHA, Limnol. Oceanogr., 41(8), 1619–1628, doi:10.4319/lo.1996.41.8.1619, 1996.

Drake, H. F., Morrison, A. K., Griffies, S. M., Sarmiento, J. L., Weijer, W., and Gray, A. R.: Lagrangian timescales of Southern Ocean upwelling in a hierarchy of model resolutions, Geophysical Research Letters, 45, 891–898, https://doi.org/10.1002/2017GL076045, 2018.

Duarte, C. M. and Agustí, S.: The CO2 Balance of Unproductive Aquatic Ecosystems, Science, 281, 234–236, https://doi.org/10.1126/science.281.5374.234, 1998.

Duce, R. A., LaRoche, J., Altieri, K., Arrigo, K. R., Baker, A. R., Capone, D. G., Cornell, S., Dentener, F., Galloway, J., Ganeshram, R. S., and Geider, R. J.: Impacts of atmospheric anthropogenic nitrogen on the open ocean, Science, 320(5878), 893-897, 2008.

Ducklow, H. W. and McCallister, S. L.: The biogeochemistry of carbon dioxide in the coastal oceans, The sea, 13, 269–315, 2004.

Dunne, J. P., Sarmiento, J. L., and Gnanadesikan, A.: A synthesis of global particle export from the surface ocean and cycling through the ocean interior and on the seafloor, Global Biogeochem. Cycles, 21, GB4006, doi:10.1029/2006GB002907, 2007.

Durand M.-H., Cury P., Mendelssohn R., Roy C., Bakun A., and Pauly D.: Global Versus Local Changes in Upwelling Systems, ORSTOM, Paris, 1998.

Emerson, S., Quay, P., Karl, D., Winn, C., Tupas, L., and Landry, M.: Experimental determination of the organic carbon flux from open-ocean surface waters, Nature, 389(6654), 951-954, 1997.

Eppley, R. W. and Peterson, B. J.: Particulate organic matter flux and planktonic new production in the deep ocean, Nature, 282(5740), 677-80, 1979.

Estrade, P., Marchesiello, P., De Verdière, A. C., and Roy, C.: Cross-shelf structure of coastal upwelling: A two dimensional extension of Ekman's theory and a mechanism for inner shelf upwelling shut down, Journal of Marine Research, 66, 589–616, doi:10.1357/002224008787536790, 2008.

Fernández, C. and Raimbault, P.: Nitrogen regeneration in the NE Atlantic Ocean and its impact on seasonal new, regenerated and export production, Marine Ecology Progress Series, 337, 79-92, 2007.

Fernández-Castro, B., Mouriño-Carballido, B., Marañón, E., Chouciño, P., Gago, J., Ramírez, T., Vidal, M., Bode, A., Blasco, D., Royer, S. J., and Estrada, M.: Importance of salt fingering for new nitrogen supply in the oligotrophic ocean, Nature communications, 6, 8002, 2015.

Fischer, G. and Karakaş, G.: Sinking rates and ballast composition of particles in the Atlantic Ocean: implications for the organic carbon fluxes to the deep ocean, Biogeosciences, 6, 85-102, 2009.

Fraile-Nuez, E., Machín, F., Vélez-Belchí, P., López-Laatzen, F., Borges, R., Benítez-Barrios, V., and Hernández-Guerra, A.: Nine years of mass transport data in the eastern boundary of the North Atlantic Subtropical Gyre, J. Geophys. Res., 115, C09009, 2010.

Frischknecht, M., Münnich, M., and Gruber, N.: Origin, Transformation, and Fate: The Three-Dimensional Biological Pump in the California Current System, Journal of Geophysical Research: Oceans, 123(11), 7939-7962, 2018.

Galbraith, E. D., Gnanadesikan, A., Dunne, J. P., and Hiscock, M. R.: Regional impacts of iron-light colimitation in a global biogeochemical model, Biogeosciences, 7, 1043–1064, https://doi.org/10.5194/bg-7-1043-2010, 2010.

Ganachaud, A. and Wunsch, C.: Oceanic nutrient and oxygen transports and bounds on export production during the World Ocean Circulation Experiment, Global Biogeochemical Cycles, 16(4), 5-1, 2002.

García-Muñoz, M., Arístegui, J., Montero, M. F. and Barton, E. D.: Distribution and transport of organic matter along a filament-eddy system in the Canaries–NW Africa coastal transition zone region, Progress in Oceanography, 62 (2-4), 115-129, 2004.

García-Muñoz, M., Arístegui, J., Pelegrí, J. L., Antoranz, A., Ojeda, A. and Torres, M.: Exchange of carbon by an upwelling filament off Cape Ghir (NW Africa), Journal of Marine Systems, 54(1-4), 83-95, 2005.

Glessmer, M.S., Eden, C. and Oschlies, A.: Contribution of oxygen minimum zone waters to the coastal upwelling off Mauritania. Progress in Oceanography, 83(1-4), pp.143-150, 2009.

Gómez-Letona, M., Ramos, A.G., Coca, J., and Arístegui, J.: Trends in primary production in the canary current upwelling system—A regional perspective comparing remote sensing models, Frontiers in Marine Science, 4, 370, 2017.

Gruber, N., and Sarmiento, J. L.: Large scale biogeochemical-physical interactions in elemental cycles, The sea, 12, 337-99, 2002.

Gruber, N., Frenzel, H., Doney, S. C., Marchesiello, P., McWilliams, J. C., Moisan, J. R., Oram, J. J., Plattner, G.-K., and Stolzenbach, K. D.: Eddy-resolving simulation of plankton ecosystem dynamics in the California Current System, Deep Sea Research Part I: Oceanographic Research Papers, 53, 1483–1516, doi:10.1016/j.dsr.2006.06.005, 2006.

Gutknecht, E., Dadou, I., Marchesiello, P., Cambon, G., Le Vu, B., Sudre, J., Garçon, V., Machu, E., Rixen, T., Kock, A., and Flohr, A.: Nitrogen transfers off Walvis Bay: a 3-D coupled physical/biogeochemical modeling approach in the Namibian upwelling system, Biogeosciences, 10(6), 4117-4135, 2013.

Hagen, E., Zulicke, C., and Feistel, R.: Near-surface structures in the Cape Ghir filament off Morocco, Oceanologica Acta, 19(6), 577–598, 1996.

Hansell, D. A. and Carlson, C. A.: Net community production of dissolved organic carbon, Global Biogeochem. Cycles, 12(3), 443–453, doi:10.1029/98GB01928, 1998.

Hansell, D. A.: DOC in the global ocean carbon cycle, Biogeochemistry of Marine Dissolved Organic Matter, Academic Press, San Diego, 685-715, 2002.

Henson, S. A., Sanders, R., Madsen, E., Morris, P. J., Le Moigne, F., and Quartly, G. D.: A reduced estimate of the strength of the ocean's biological carbon pump, Geophys. Res. Lett., 38, L04606, doi:10.1029/2011GL046735, 2011.

Hernández-Guerra, A., Fraile-Nuez, E., López-Laatzen, F., Martínez, A., Parrilla, G., and Vélez-Belchí, P.: Canary Current and North Equatorial Current from an inverse box model, Journal of Geophysical Research: Oceans, 110(C12), 2005.

Holzer, M. and Primeau, F. W.: The path-density distribution of oceanic surface-to-surface transport, Journal of Geophysical Research: Oceans, 113(C1), 2008.

Hyde, K., O'Reilly, J., and Oviatt, C.: Validation of SeaWiFS chlorophyll-a in Massachusetts Bay, Cont. Shelf Res., 27, 1677–1691, 2007.

Jahnke, R.A., Reimers, C.E., and Craven, D.B.: Intensification of recycling of organic matter at the sea floor near ocean margins, Nature, 348, 50–53, 1990.

Jahnke, R.A.: The global ocean flux of particulate organic carbon: areal distribution and magnitude, Global Biogeochemistry Cycles, 10, 71–88, 1996.

Kämpf, J., and Chapman, P.: The Canary/Iberia Current Upwelling System, in: Upwelling Systems of the World, Springer, Cham, 203-250, 2016.

Klenz, T., Dengler, M., Brandt, P.: Seasonal variability of the Mauritania Current and hydrography at 18°N. Journal of Geophysical Research: Oceans, 123, 8122– 8137, https://doi.org/10.1029/2018JC014264, 2018.

Kounta, L., Capet, X., Jouanno, J., Kolodziejczyk, N., Sow, B., and Gaye, A. T.: A model perspective on the dynamics of the shadow zone of the eastern tropical North Atlantic – Part 1: the poleward slope currents along West Africa, Ocean Sci., 14, 971–997, https://doi.org/10.5194/os-14-971-2018, 2018.

Lachkar, Z.: Effects of upwelling increase on ocean acidification in the California and Canary Current systems, Geophysical Research Letters, 41, 90–95, doi:10.1002/2013GL058726, 2014.

Lachkar, Z. and Gruber, N.: What controls biological production in coastal upwelling systems? Insights from a comparative modeling study, Biogeosciences, 8, 2961-2976, 2011.

Lachkar, Z. and Gruber, N.: Response of biological production and air-sea CO2 fluxes to upwelling intensification in the California and Canary Current Systems, Journal of Marine Systems, 109-110, 149–160, doi:10.1016/j.jmarsys.2012.04.003, 2013.

Lachkar, Z., Smith, S., Lévy, M., and Pauluis, O.: Eddies reduce denitrification and compress habitats in the Arabian Sea, Geophys. Res. Lett., 43, 9148–9156, doi:10.1002/2016GL069876, 2016.

Large, W.G., McWilliams, J.C., and Doney, S.C.: Oceanic vertical mixing: A review and a model with a nonlocal boundary layer parameterization, Reviews of Geophysics, 32(4), 363-403, 1994.

Large, W. G., and Danabasoglu, G.: Attribution and Impacts of Upper-Ocean Biases in CCSM3. J. Climate, 19, 2325–2346, https://doi.org/10.1175/JCLI3740.1, 2006.

Laws, E. A., Falkowski P. G., Smith W. O., Ducklow H., and McCarthy J. J.: Temperature effects on export production in the open ocean, Global Biogeochem. Cycles, 14(4), 1231–1246, doi:10.1029/1999GB001229, 2000.

Le Moigne, F. A., Henson, S. A., Sanders, R. J., and Madsen, E.: Global database of surface ocean particulate organic carbon export fluxes diagnosed from the 234 Th technique, Earth System Science Data, 5(2), 295-304, 2013.

Lin, J., Brunner, D., Gerbig, C., Stohl, A., Luhar, A. and Webley, P.: Lagrangian modeling of the atmosphere, vol. 200 of Geophysical Monograph Series. American Geophysical Union, Washington DC, 5, 2012.

Liu, K. K., Iseki, K., and Chao, S. Y.: Continental margin carbon fluxes, The changing ocean carbon cycle: a midterm synthesis of the Joint Global Ocean Flux Study, 5, 2000.

Liu, K. K., Atkinson, L., Quinones, R., and Talaue-McManus, L.: Biogeochemistry of Continental Margins in a global Context, Carbon and Nutrient Fluxes in Continental Margins. 2–24, doi:10.1007/978-3-540-92735-, 2010.

Longhurst, A. R.: Ecological Geography of the Sea, Academic Press, San Diego, 2007.

Lovecchio, E., Gruber, N., Münnich, M., and Lachkar, Z.: On the long-range offshore transport of organic carbon from the Canary Upwelling System to the open North Atlantic, Biogeosciences, 14, 3337, 2017.

Lovecchio, E., Gruber, N., and Münnich, M.: Mesoscale contribution to the long-range offshore transport of organic carbon from the Canary Upwelling System to the open North Atlantic, Biogeosciences, 15(16), 5061-5091, 2018.

Lozier, S. M., Owens, S. B., and Curry, R. G.: The climatology of the North Atlantic, Prog. Oceanogr., 36, 1-44, 1995.

Lumpkin, R. and Johnson, G. C.: Global ocean surface velocities from drifters: Mean, variance, El Niño–Southern Oscillation response, and seasonal cycle, Journal of Geophysical Research: Oceans, 118(6), 2992-3006, 2013.

Luo, Y. W., Doney, S. C., Anderson, L. A., Benavides, M., Berman-Frank, I., Bode, A., Bonnet, S., Boström, K. H., Böttjer, D., Capone, D. G., and Carpenter, E. J.: Database of diazotrophs in global ocean: abundance, biomass and nitrogen fixation rates, Earth System Science Data, 4(1), 47-73, 2012.

Machín, F., Pelegrí, J. L., Marrero-Díaz, A., Laiz, I., and Ratsimandresy, A. W.: Near-surface circulation in the southern Gulf of Cádiz, Deep-Sea Res., 53, 1161-1181, 2006.

Mahaffey C., Williams R. G., Wolff G. A., and Anderson W. T.: Physical supply of nitrogen to phytoplankton in the Atlantic Ocean, Global Biogeochemical Cycles, Mar 1, 18(1), 2004.

Marchesiello, P., McWilliams, J. C., and Shchepetkin, A.: Equilibrium Structure and Dynamics of the California Current System, Journal of Physical Oceanography, 33, 753–783, doi:10.1175/1520-0485(2003)33<753:ESADOT>2.0.CO;2, 2003.

Marchesiello, P., Debreu, L., and Couvelard, X.: Spurious diapycnal mixing in terrain-following coordinate models: The problem and a solution, Ocean Modelling, 26(3-4), 156-169, 2009.

Martel, F. and Wunsch, C.: The North Atlantic circulation in the early 1980s-An estimate from inversion of a finite-difference model, Journal of Physical Oceanography, 23(5), 898-924, 1993.

Mason, E., Colas, F., Molemaker, J., Shchepetkin, A. F., Troupin, C., McWilliams, J. C., and Sangrà, P.: Seasonal variability of the Canary Current: a numerical study, J. Geophys. Res., 116, C06001, 2011.

Mason, E., Colas, F. , and Pelegrí, J. L.: A Lagrangian study tracing water parcel origins in the Canary Upwelling System. Scientia Marina, 76(S1), 79-94, 2012.

Meunier, T., Rossi, V., Morel, Y. and Carton, X.: Influence of bottom topography on an upwelling current: Generation of long trapped filaments. Ocean Modelling, 35(4), 277-303, 2010.

Mittelstaedt, E.: The upwelling area off Northwest Africa—A description of phenomena related to coastal upwelling, Progress in Oceanography, 12, 307–331, doi:10.1016/0079-6611(83)90012-5, 1983.

Mittelstaedt, E.: The ocean boundary along the northwest African coast: Circulation and oceanographic properties at the sea surface, Progress in Oceanography, 26(4), 307-355, 1991.

Mittelstaedt, E. and Hamann, I.: The coastal circulation off Mauritania, Deutsche Hydrographische Zeitschrift, 34, 81–118, doi:10.1007/BF02226483, 1981.

Moreira-Coello, V., Mouriño-Carballido, B., Marañón, E., Fernández-Carrera, A., Bode, A., and Varela, M.M.: Biological N2 fixation in the upwelling region off NW Iberia: magnitude, relevance, and players, Frontiers in Marine Science, 4, 303, 2017.

Moore, J. K., Doney, S. C., and Lindsay, K.: Upper ocean ecosystem dynamics and iron cycling in a global three-dimensional model, Global Biogeochem. Cy., 18, GB4028, https://doi.org/10.1029/2004GB002220, 2004.

Moore, C. M., Mills, M. M., Achterberg, E. P., Geider, R. J., LaRoche, J., Lucas, M. I., McDonagh, E. L., Pan, X., Poulton, A. J., Rijkenberg, M. J., and Suggett, D. J.: Large-scale distribution of Atlantic nitrogen fixation controlled by iron availability, Nature Geoscience, 2(12), 867-871, 2009.

Moore, C. M., Mills, M.M., Arrigo, K.R., Berman-Frank, I., Bopp, L., Boyd, P.W., Galbraith, E.D., Geider, R.J., Guieu, C., Jaccard, S.L., and Jickells, T.D.: Processes and patterns of oceanic nutrient limitation, Nature geoscience, 6(9), 701-710, 2013.

Muller-Karger, F. E., Varela, R., Thunell, R., Luerssen, R., Hu, C., and Walsh, J. J.: The importance of continental margins in the global carbon cycle, Geophysical research letters, 32(1), 2005.

Nagai, T., Gruber, N., Frenzel, H., Lachkar, Z., McWilliams, J. C., and Plattner, G. K.: Dominant role of eddies and filaments in the offshore transport of carbon and nutrients in the C alifornia C urrent S ystem, Journal of Geophysical Research: Oceans, 120(8), 5318-5341, 2015.

Ndoye, S., X. Capet, P. Estrade, B. Sow, E. Machu, T. Brochier, J. Döring, and P. Brehmer: Dynamics of a "low-enrichment high-retention" upwelling center over the southern Senegal shelf, Geophys. Res. Lett., 44, 5034– 5043, doi:10.1002/2017GL072789, 2017.

Pastor, M. V., Palter, J. B., Pelegrí, J. L., and Dunne, J. P.: Physical drivers of interannual chlorophyll variability in the eastern subtropical North Atlantic, Journal of Geophysical Research: Oceans, 118(8), 3871-3886, 2013.

Pauly, D. and Christensen, V.: Primary production required to sustain global fisheries, Nature, 374(6519), 255-257, 1995.

Pelegri, J. L., Arístegui, J., Cana, L., González, M., Hernández-Guerra, A., Hernández-León, S., Marrero-Díaz, A., Montero, M. F., Sangrá, P., and Santana-Casiano, M.: Coupling between the open ocean and the coastal upwelling region off Northwest Africa: Water recirculation and offshore pumping of organic matter, J. Mar. Syst., 54, 3-37, 2005a.

Pelegri, J. L., Marrero-Dıaz, A., Ratsimandresy, A., Antoranz, A., Cisneros-Aguirre, J., Gordo, C., Grisolıa, D., Hernandez-Guerra, A., Laiz, I., Martınez, A., Parrilla1, G., Perez-Rodrıguez, P., Rodrıguez-Santana, A., and Sangra, P.: Hydrographic cruises off northwest Africa: the Canary Current and the Cape Ghir region, Journal of Marine Systems, 54, 39 – 63, 2005b.

Pelegri, J. L., Marrero-Díaz, A., and Ratsimandresy, A. W.: Nutrient irrigation of the North Atlantic, Prog. Oceanogr., 70 (2-4), 366-406, 2006.

Pelegri, J. L. and Benazzouz, A.: Coastal upwelling off North-West Africa, 2015.

Peliz, Á., Santos, A. M. P., Oliveira, P. B., and Dubert, J.: Extreme cross-shelf transport induced by eddy interactions southwest of Iberia in winter 2001, Geophysical Research Letters, 31(8), 2004.

Price, J. F., Baringer, M. O. N., Lueck, R. G., Johnson, G. C., Ambar, I., Parrilla, G., Cantos, A., Kennelly, M. A., and Sanford, T.B.: Mediterranean outflow mixing and dynamics, Science, 259(5099), 1277-1282, 1993.

Risien, C. M. and Chelton, D. B.: A global climatology of surface wind and wind stress fields from eight years of QuikSCAT scatterometer data, Journal of Physical Oceanography, 38(11), 2379-2413, 2008.

Rivas, D. and Samelson, R.M.: A numerical modeling study of the upwelling source waters along the Oregon coast during 2005, Journal of Physical Oceanography, 41(1), 88–112, 2011.

Rykaczewski R. R., Checkley D. M. Jr.: Influence of ocean winds on the pelagic ecosystem in upwelling regions, Proc. Natl. Acad. Sci, 105, 1965-1970, 2008.

Sangrà, P., Pascual, A., Rodríguez-Santana, Á., Machín, F., Mason, E., McWilliams, J. C., Pelegrí, J. L., Dong, C., Rubio, A., Arístegui, J., and Marrero-Díaz, Á.: The Canary Eddy Corridor: A major pathway for long-lived eddies in the subtropical North Atlantic, Deep Sea Research Part I: Oceanographic Research Papers. 56.12, 2100-2114, 2009.

Santana-Falcón, Y., Benavides, M., Sangrà, P., Mason, E., Barton, E. D., Orbi, A., and Arístegui, J.: Coastal–offshore exchange of organic matter across the Cape Ghir filament (NW Africa) during moderate upwelling, Journal of Marine Systems, 154, 233-242, 2016.

Sarmiento, J. L., Herbert, T., and Toggweiler, J. R.: Mediterranean nutrient balance and episodes of anoxia, Global Biogeochemical Cycles, 2(4), 427-444, 1988.

Schlitzer, R.: Export production in the equatorial and North Pacific derived from dissolved oxygen, nutrient and carbon data, J. Oceanogr., 60(1), 53–62, doi:10.1023/B:JOCE.0000038318.38916.e6, 2004.

Schollaert, S. E., Yoder, J. A., O'Reilly, J. E., and Westphal, D. L.: Influence of dust and sulfate aerosols on ocean color spectra and chlorophyll a concentrations derived from SeaWiFS off the US east coast, J. Geophys. Res., 108, 3191, 1–13, doi:10.1029/2000JC000555, 2003.

Schütte, F., Brandt, P., and Karstensen, J.: Occurrence and characteristics of mesoscale eddies in the tropical northeastern Atlantic Ocean, Ocean Sci., 12, 663–685, https://doi.org/10.5194/os-12-663-2016, 2016.

Shchepetkin, A. F. and McWilliams, J. C.: The regional oceanic modeling system (ROMS): a split-explicit, free-surface, topography-following-coordinate oceanic model, Ocean Modelling, 9, 347–404, 2005.

Shigemitsu, M., Okunishi, T., Nishioka, J., Sumata, H., Hashioka, T., Aita, M. N., Smith, S. L., Yoshie, N., Okada, N., and Yamanaka, Y.: Development of a one-dimensional ecosystem model including the iron cycle applied to the Oyashio region, western subarctic Pacific, J. Geophys. Res.-Oceans, 117, c06021, https://doi.org/10.1029/2011JC007689, 2012.

Siegel, D. A., Buesseler, K. O., Doney, S. C., Sailley, S. F., Behrenfeld, M. J., and Boyd, P. W.: Global assessment of ocean carbon export by combining satellite observations and food-web models, Global Biogeochemical Cycles, 28(3), 181–196, 2014.

Smith, S. and Hollibaugh, J. T.: Coastal Metabolism and the Oceanic Organic Carbon Balance, Reviews of Geophysics, 31, 75–89, doi:10.1029/92RG02584, 1993.

Smith, W. H. and Sandwell, D. T.: Global sea floor topography from satellite altimetry and ship depth soundings, Science, 277(5334), 1956-1962, 1997.

Smyth, T., Quartly, G., Jackson, T., Tarran, G., Woodward, M., Harris, C., Gallienne, C., Thomas, R., Airs, R., Cummings, D., and Brewin, R.: Determining Atlantic Ocean province contrasts and variations, Progress in Oceanography, 158, 19-40, 2017.

Stramma, L.: Geostrophic transport in the warm water sphere of the eastern subtropical North Atlantic, J. Mar. Res., 42, 537-558, 1984.

Taylor, K. E.: Summarizing multiple aspects of model performance in a single diagram, Journal of Geophysical Research: Atmospheres, 106(D7), 7183-7192, 2001.

Tilstone, G., Smyth, T., Poulton, A., and Hutson, R.: Measured and remotely sensed estimates of primary production in the Atlantic Ocean from 1998 to 2005, Deep Sea Research Part II: Topical Studies in Oceanography, 56(15), 918-930, 2009.

Troupin, C., Mason, E., Beckers, J.M. and Sangrà, P.: Generation of the Cape Ghir upwelling filament: A numerical study. Ocean Modelling, 41, 1-15, 2012.

Van Camp, L., Nykjaer, L., Mittelstaedt, E., and Schlittenhardt, P.: Upwelling and boundary circulation off northwest Africa as depicted by infrared and visible satellite observations, Prog. Oceanogr., 26, 357-402, 1991.

Van Sebille, E., Griffies, S.M., Abernathey, R., Adams, T.P., Berloff, P., Biastoch, A., Blanke, B., Chassignet, E.P., Cheng, Y., Cotter, C.J. and Deleersnijder, E.: Lagrangian ocean analysis: Fundamentals and practices. Ocean Modelling, 121, pp.49-75, 2018.

Varela, M., Bode, A., Fernandez, E., Gonzalez, N., Kitidis, V., and Woodward, E. M. S.: Nitrogen uptake and dissolved organic nitrogen release in planktonic communities characterised by phytoplankton size–structure in the Central Atlantic Ocean, Deep Sea Research Part I: Oceanographic Research Papers, 52(9), 1637-1661, 2005.

Walsh, J. J.: Importance of Continental Margins in the Marine Biogeochemical Cycling of Carbon and Nitrogen, Nature, 350, 53–55, doi:10.1038/350053a0, 1991.

Westberry, T., Behrenfeld, M. J., Siegel, D. A., and Boss, E.: Carbon-based primary productivity modeling with vertically resolved photoacclimation, Global Biogeochem. Cycles, 22, GB2024, doi:10.1029/2007GB003078, 2008.

Williams, R. G. and Follows, M. J.: The Ekman transfer of nutrients and maintenance of new production over the North Atlantic, Deep Sea Res., Part I, 45, 461–489, 1998.

Wollast, R.: Evaluation and comparison of the global carbon cycle in the coastal zone and in the open ocean, The sea, 10, 213–252, 1998.

Yool, A., Martin, A. P., Fernandez, C., and Clark, D. R.: The significance of nitrification for oceanic new production, Nature, 447(7147), 999–1002, doi:10.1038/nature05885, 2007.